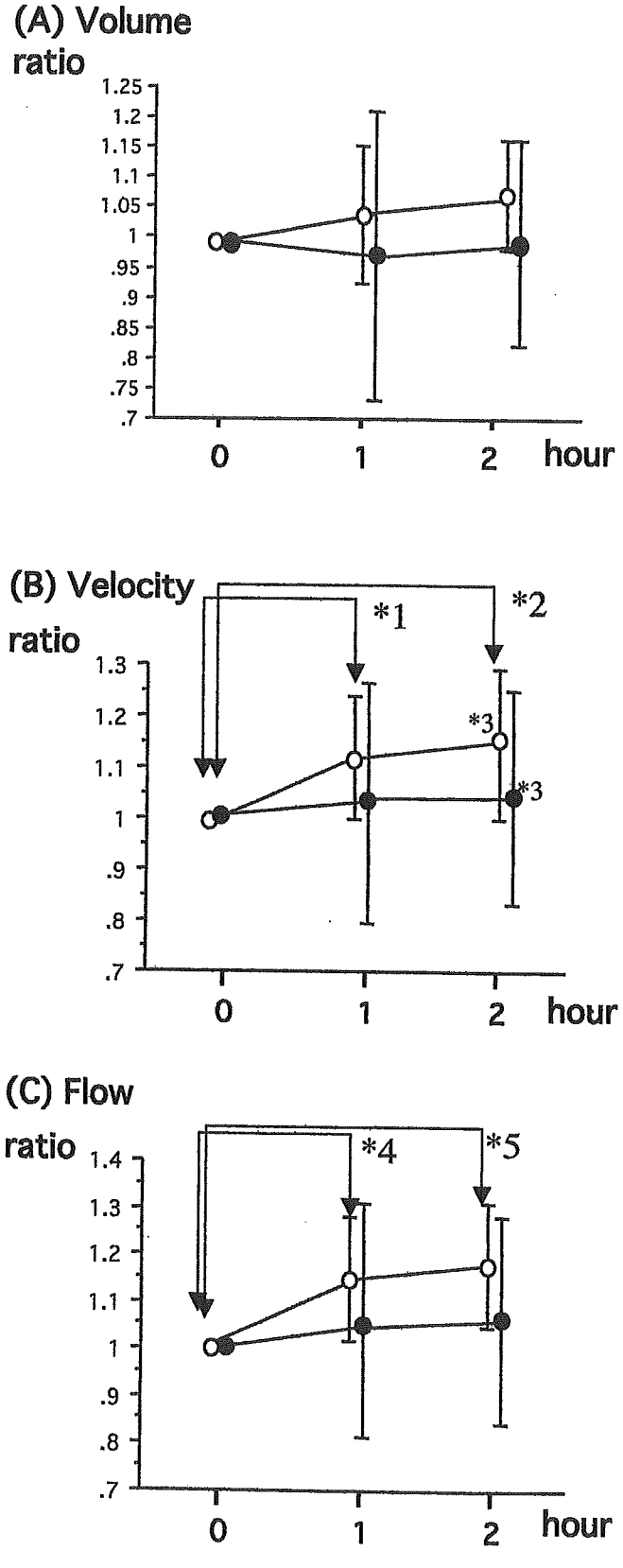

It has been reported that the peak concentration of unoprostone in plasma is attained at 20 min (38 ng/g wet tissue) after instillation in rabbit eyes, and a rapid reduction is observed after 1 h. Corresponding concentration changes have been observed in different tissues of the fellow eyes.[3] These results support our observations of a contralateral effect at 1 h after instillation in NTG patients (Study 2). However, the results of these other studies were obtained in rabbit eyes, and our results in human eyes did not show a statistically significant difference. The lack of a significant difference between eyes treated with unoprostone and eyes treated with placebo in NTG patients might also be explained by the contralateral effect.

The vascular endothelium plays a vital role in the control of blood flow. It releases factors such as endothelin (ET)-1, which can contract the vascular smooth muscles in the blood vessels, or nitric oxide, which can relax the muscles. In NTG patients, the level of plasma ET-1 is significantly higher than the level in normal volunteers,[29] and ET-1 can induce a reduction in blood flow in the ONH and choroid by its strong vasopressor effect and induction of smooth muscle contraction. In rabbits with chronic ONH ischemia created by repeated intravitreal injection of ET-1, the ratio of cup area to disc area is significantly increased, and histologic examination shows axonal loss and demyelination affecting the prelaminar portion of the optic nerve independently of the IOP level.[30]

The capability of unoprostone to antagonize the effects of ET-1 has been reported.[31–34] Unoprostone almost completely inhibits ET-induced contractions of bovine trabecular meshwork and ciliary muscle by blocking the ET-induced increase in intracellular calcium levels, although it has no effect on baseline intracellular calcium levels.[33] Unoprostone has also been shown to improve the circulation in the optic disc of animals treated with ET-1.[19] Because elevated ET-1 is found in NTG patients and may be responsible for the decreased blood flow in the ONH, unoprostone, a strong antagonist of ET-1, may be a new candidate medication for the treatment of NTG patients.

In conclusion, the effects of unoprostone demonstrated in this study suggest that it improves blood flow in the ONH mainly by opposing ET-induced blood flow reduction, which may lead to advantages in treating glaucoma patients, especially NTG patients, whose plasma concentration of ET-1 has been reported to be higher than normal.

Figure 2A–C. Ratios of blood volume, velocity, and flow relative to baseline values in unoprostone-treated group (*open circles*) and control group (*closed circles*) of normal subjects. Each point and error bar represents the mean ± SD. **A** Volume ratio. There were no significant changes in the volume ratio in either group. **B** Velocity ratio. Velocity in subjects treated with unoprostone increased by 11.1% (**1*, $P = 0.0059$) at 1 h and 16.2% (**2*, $P = 0.001$) at 2 h after instillation. A comparison between groups treated with unoprostone versus placebo showed that velocity was significantly higher in the unoprostone-treated eyes 2 h after instillation (**3*, $P = 0.0266$). **C** Flow ratio. Flow in subjects treated with unoprostone increased by 11.6% (**4*, $P = 0.0041$) at 1 h and 14.7% (**5*, $P = 0.0004$) at 2 h after instillation.

Jpn J Ophthalmol
Vol 49: 287–293, 2005

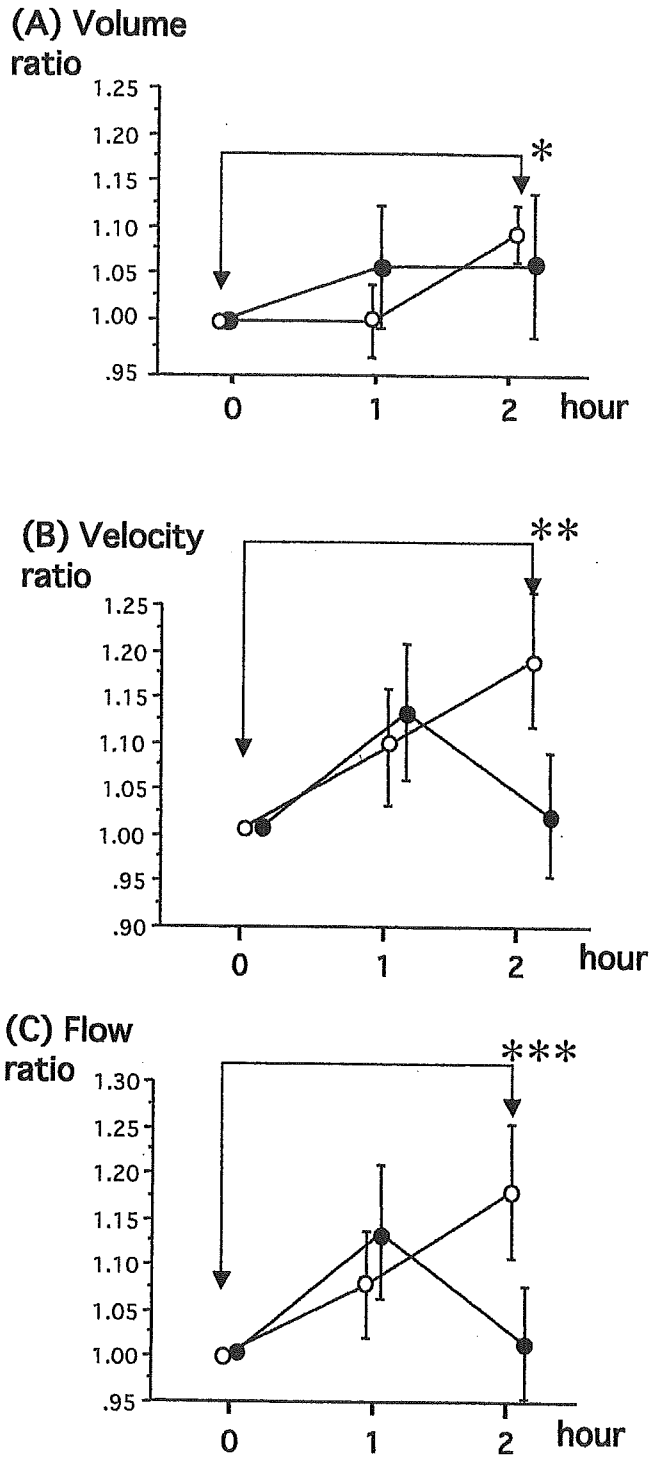

Figure 3A–C. The ratios of blood volume, velocity, and flow relative to baseline values of unoprostone treated eyes (*open circles*) and control eyes (*closed circles*) in normal-tension glaucoma (NTG) patients. Each point and error bar represents the mean ± SD. **A** Volume ratio. Volume increased by 9.6% at 2 h after instillation ($*P = 0.0282$) in eyes treated with unoprostone. **B** Velocity ratio. Velocity in eyes treated with unoprostone increased by 17.3% at 2 h after instillation ($**P = 0.0289$). **C** Flow ratio. Flow increased by 18.2% at 2 h after instillation ($***P = 0.0250$) in eyes treated with unoprostone.

Acknowledgments. This study was supported by the Keio University Medical Science Fund Research Grants for Life Sciences and Medicine, and the Keio Health Counseling Center. The unoprostone isopropyl and unoprostone isopropyl vehicle solution used in this study were supplied without charge by Fujisawa Pharmaceutical Company, Osaka, Japan.

References

1. Taniguchi T, Haque MS, Sugiyama K, Hori N, Kitazawa Y. Ocular hypotensive mechanism of topical isopropyl unoprostone, a novel prostaglandin metabolite-related drug, in rabbits. J Ocul Pharmacol Ther 1996;12:489–498.
2. Ueno R, Yoshida S, Deguchi T, et al. The intraocular pressure lowering effects of UF-21, a novel prostaglandin-related compound, in animals. Nippon Ganka Gakkai Zasshi (Acta Soc Ophthalmol Jpn) 1992;96:462–468.
3. Watanabe C, Matsumoto S, Kin K, Tsuchisaka H, Ueno R. Ocular penetration of UF-21, a new prostaglandin-related compound, in the rabbit eye. Nippon Ganka Gakkai Zasshi (Acta Soc Ophthalmol Jpn) 1992;96:335–339.
4. Azuma I. Clinical evaluations of UF-21 ophthalmic solution in glaucoma patients refractory to maximum tolerable therapy. Nippon Ganka Gakkai Zasshi (Acta Soc Ophthalmol Jpn) 1993;97:232–238.
5. Azuma I, Masuda K, Kitazawa Y, Takase M, Yamamura H. Double-masked comparative study of UF-21 and timolol ophthalmic solutions in patients with primary open-angle glaucoma or ocular hypertension. Jpn J Ophthalmol 1993;37:514–525.
6. Stewart WC, Stewart JA, Crockett S, Kubilus C, Brown A, Shams N. Comparison of the cardiovascular effects of unoprostone 0.15%, timolol 0.5% and placebo in healthy adults durinq exercise using a treadmill test. Acta Ophthalmol Scand 2002:80:272–276.
7. Ohtake Y, Tanino T, Kimura I, Mashima Y, Oguchi Y. Lonq-term efficacy and safety of combined topical antiglaucoma therapy—timolol & unoprostone vs. betaxolol & unoprostone. Nippon Ganka Gakkai Zasshi (J Jpn Ophthalmol Soc) 2004:108:23–28.
8. Sakurai M, Araie M, Oshika T, Mori M, Shoji N, Masuda K. Effects of topical application of UF-021, a novel prostaglandin derivative, on aqueous humor dynamics in normal human eyes. Jpn J Ophthalmol 1993;37:252–258.
9. Takase M, Murao M, Koyano S, Okita M, Ueno R. Ocular effects of continuous topical instillations of UF-21 ophthalmic solution in healthy volunteers. Nippon Ganka Gakkai Zasshi (Acta Soc Ophthalmol Jpn) 1992;96:1261–1267.
10. Tetsuka H, Tsuchisaka H, Kin K, Takahashi Y, Takase M. A mechanism for reducing intraocular pressure in normal tension volunteers using UF-021, a prostaglandin-related compound. Nippon Ganka Gakkai Zasshi (Acta Soc Ophthalmol Jpn) 1992;96: 496–500.
11. Nordmann JP, Rouland JF, Mertz BP. A comparison of the intraocular pressure-lowering effect of 0.5% timolol maleate and the docosanoid derivative of a PGF2a metabolite, 0.12% unoprostone, in subjects with chronic open-angle glaucoma or ocular hypertension. Curr Med Res Opin 1999;15:87–93.
12. Stewart WC, Stewart JA, Kapic BM. The effects of unoprostone isopropyl 0.12% and timolol maleate 0.5% on diurnal intraocular pressure. J Glaucoma 1998;7:388–394.
13. Day DG, Schacknow PN, Wand M, et al. Timolol 0.5%/dorzolamide 2% fixed combination vs. timolol maleate 0.5% and unoprostone 0.15% given twice daily to patients with primary open-angle glaucoma or ocular hypertension. Am J Ophthalmol 2003;135:138–143.
14. Hommer A, Kapik B, Shams N, The Unoprostone Adjunctive Therapy Study Group. Unoprostone as adjunctive therapy to timolol: a double-masked randomised study versus brimonidine and dorzolamide. Br J Ophthalmol 2003;87:592–598.
15. Flammer J, Drance SM. The effect of a number of glaucoma medications on the differential light threshold. Doc Ophthalmol Proc Ser 1983;35:146–148.

16. Flammer J, Drance SM. Influence of pindolol and timolol treatment on the visual fields of glaucoma patients. J Ocul Pharmacol 1986;2:305–311.
17. Kidd MN, O'Connor M. Progression of field loss after trabeculectomy: a five-year follow up. Br J Ophthalmol 1985;69: 827–831.
18. Schulzer M, Mikelberg FS, Drance SM. Some observations on the relation between intraocular pressure reduction and the progression of glaucomatous visual loss. Br J Ophthalmol 1987;71: 486–488.
19. Sugiyama T, Azuma I. Effect of UF-21 on optic nerve head circulation in rabbits. Jpn J Ophthalmol 1995;39:124–129.
20. Broadway D, Drance SM. Glaucoma and vasospasm. Br J Ophthalmol 1998;82:862–870.
21. Carter CJ, Brooks DE, Doyle DL, Drance SM. Investigations into a vascular etiology for low-tension glaucoma. Ophthalmology 1990;97:49–55.
22. Flammer J. The vascular concept of glaucoma. Surv Ophthalmol 1994;38:53–56.
23. Hitchings R. Low-tension glaucoma—its place in modern glaucoma practice. Br J Ophthalmol 1992;76:494–496.
24. Levene R. Low-tension glaucoma: a critical review and new material. Surv Ophthalmol 1980;24:621–664.
25. Michelson G, Schmauss B. Two-dimensional mapping of the perfusion of the retina and optic nerve head. Br J Ophthalmol 1995;79: 1126–1132.
26. Michelson G, Schmauss B, Langhans MJ, Harazny J, Groh MJ. Principle, validity, and reliability of scanning laser Doppler flowmetry. J Glaucoma 1996;5:99–105.
27. Bohdanecka Z, Orgul S, Purunte C, Flammer J. Influence of acquisition parameters on hemodynamic measurements with the Heidelberg retina flowmeter at the optic disc. J Glaucoma 1998;7: 151–157.
28. Chauhan BC, Smith PM. Confocal scanning laser Doppler flowmetry: experiments in a model flow system. J Glaucoma 1997;13: 225–233.
29. Sugiyama T, Moriya S, Oku H, Azuma I. Association of endothelin-1 with normal tension glaucoma: clinical and fundamental studies. Surv Ophthalmol 1995;39:S49–56.
30. Oku H, Sugiyama T, Kojima S, Watanabe T, Azuma I. Experimental optic cup enlargement caused by endothelin-1-induced chronic optic nerve head ischemia. Surv Ophthalmol 1999;44:S74–84.
31. Ishii K, Araie M. Effect of topical isopropyl unoprostone (Rescula@) on tissue circulation of optic nerve head in cynomolgus monkeys. Nihon Ganka Kiyo (Folia Ophthalmol Jpn) 1999; 50:224–228.
32. Yu DY, Su EN, Cringle SJ, Schoch C, Percicot CP, Lambrou GN. Comparison of the vasoactive effects of the docosanoid unoprostone and selected prostanoids on isolated perfused retinal arterioles. Invest Ophthalmol Vis Sci 2001;42:1499–1504.
33. Thieme H, Stumpff F, Ottlecz A, Percicot CL, Lambrou GN, Wiederholt M. Mechanisms of action of unoprostone on trabecular meshwork contractility. Invest Ophthalmol Vis Sci 2001;42: 3193–3201.
34. Hollo G, Visontai Z, Lakatos P, Vargha P. Unoprostone isopropyl pretreatment decreases endothelin-1 release and the intra-ocular pressure spike induced by laser trabeculoplasty in the rabbit. Ophthalmologica 2003;217:231–236.

and colleagues,[6] who observed a diffuse retinal pigment epithelium–choriocapillaris thickening with nodular features in the macular area. Foveal thickness was preserved, from 121 to 200 μm (mean 144 μm; SD 38.2 μm) (Table), except in patient 1's left eye (best-corrected visual acuity 20/200; 72 μm).

This morphologic preservation probably explained the relative conservation of best-corrected visual acuity of our patients despite the importance of the lesions observed in the fundus. Retinal thickness above the large drusen also appeared well preserved above drusen, although there were some waves of the surface of the retina ranging 221 to 292 μm (mean 260 μm, SD 24.7). The small peripheral radial drusen could not be clearly identified either on OCT1 or OCT3. In patient 4's right eye, the retinal pigment epithelium and the Bruch membrane seemed to be dissociated, with an accumulation of a hyporeflective fluid between both layers (Figure 2, left). One hypothesis could be that these drusen, or a lipidic component amalgamated with Bruch membrane, create a hydrophobic barrier between retinal pigment epithelium and Bruch membrane, leading to an accumulation of fluid between both layers.[7] Despite this dissociation, Bruch membrane was still reflective, containing hyperreflective elevations on its internal side. In patient 4, localized elevations of the drusen were more rarely visible than in other patients, which is consistent with the hypothesis of a confluence of the drusen in this patient (Figure 2).

In conclusion, the large paracentral drusen observed in these patients with ML presented either as a thickening of the retinal pigment epithelium–Bruch complex or as local limited elevation of retinal pigment epithelium–Bruch complex. Remarkable preservation of the neurosensory retina was observed in both foveal and perimacular areas.

REFERENCES

1. Vogt A. Die Ophthalmoskopie im rotfreien licht. In: Graefe A, Saemisch T, editors. Handbuch der gesammten augenheilkunde: untersuchungsmethoden, 3rd ed. Berlin: Verlag von Wilhelm Engelman, 1925:1–118.
2. Doyne RW. Peculiar condition of choroiditis occurring in several members of the same family. Trans Ophthalmol Soc UK 1899;19:71.
3. Stone EM, Lotery AJ, Munier FL, et al. A single *EFEMP1* mutation associated with both malattia leventinese and Doyne honeycomb retinal dystrophy. Nat Genet 1999;22:199–202.
4. Holz FG, Owens SL, Marks J, Haimovici R, Bird AC. Ultrastructural findings in autosomal dominant drusen. Arch Ophthalmol 1997;115:788–792.
5. Marmorstein LY, Munier FL, Arsenijevic Y, et al. Aberrant accumulation of *EFEMP1* underlies drusen formation in malattia leventinese and age-related macular degeneration. Proc Natl Acad Sci U S A 2002;99:13067–13072.
6. Gaillard MC, Wolfensberger TJ, Uffer S, et al. Optical coherence tomography in malattia leventinese. Klin Monatsbl Augenheilkd 2005;222:180–185.
7. Pauleikhoff D, Zuels S, Sheraidah GS, Marshall J, Wessing A, Bird AC. Correlation between biochemical composition and fluorescein binding of deposits in Bruch's membrane. Ophthalmology 1992;99:1548–1553.

Subjective Visual Sensation During Vitrectomy Under Retrobulbar Anesthesia

Nanae Kawaguchi, MD, Makoto Inoue, MD, Eiko Sugimura, MD, Kei Shinoda, MD, and Kazuo Tsubota, MD

PURPOSE: To report a precise illustrated image of patient's view during vitrectomy.

DESIGN: Interventional case report.

METHODS: >A 56-year-old male with cystoid macular edema (CME) associated with epiretinal membrane underwent vitrectomy. The patient seemed to find gratification in being operated on because he was able to see what was going on. He was a professional artist in computer graphics, and he drew three different pictures depending on the surgical procedures.

RESULTS: These pictures depicted the moving of pasty, whirling fluid during core vitrectomy, numerous black or gray spots like snowflakes by intravitrealy injected crystals of triamcinolone acetonide, and a sharp tapered instrument coming into the center and membrane-like material being peeled off.

CONCLUSIONS: Patients may see a precise shape in a constant size, scale, and detailed movement as well, focused on the retina without described optics. Further investigation will be required to determine this mechanism. (Am J Ophthalmol 2006;141:407–409. © 2006 by Elsevier Inc. All rights reserved.)

PATIENTS HAVE REPORTED VISUAL SENSATIONS PERceived during cataract surgery.[1–3] These patients experience a wide variety of visual sensations, including flashing white and/or colored lights, moving objects, instruments, and the surgeon's fingers or hands. However, these visual sensations during vitrectomy have been verbal descriptions. We performed vitrectomy on a professional artist in computer graphics, who provided us with detailed drawings of his visual sensations during surgery.

Accepted for publication Sep 6, 2005.

From the Department of Ophthalmology, Keio University School of Medicine, Tokyo, Japan (N.K., M.I., E.S., K.S., K.T.); and Laboratory of Visual Physiology, National Institute of Sensory Organs, Tokyo, Japan (K.S.).

Inquiries to Kei Shinoda, MD, Department of Ophthalmology, Keio University, School of Medicine, 35 Shinanomachi, Shinjyuku-ku, Tokyo, 160-8582, Japan; fax: (+81) 33359-8302; e-mail: shinodak@sc.itc.keio.ac.jp

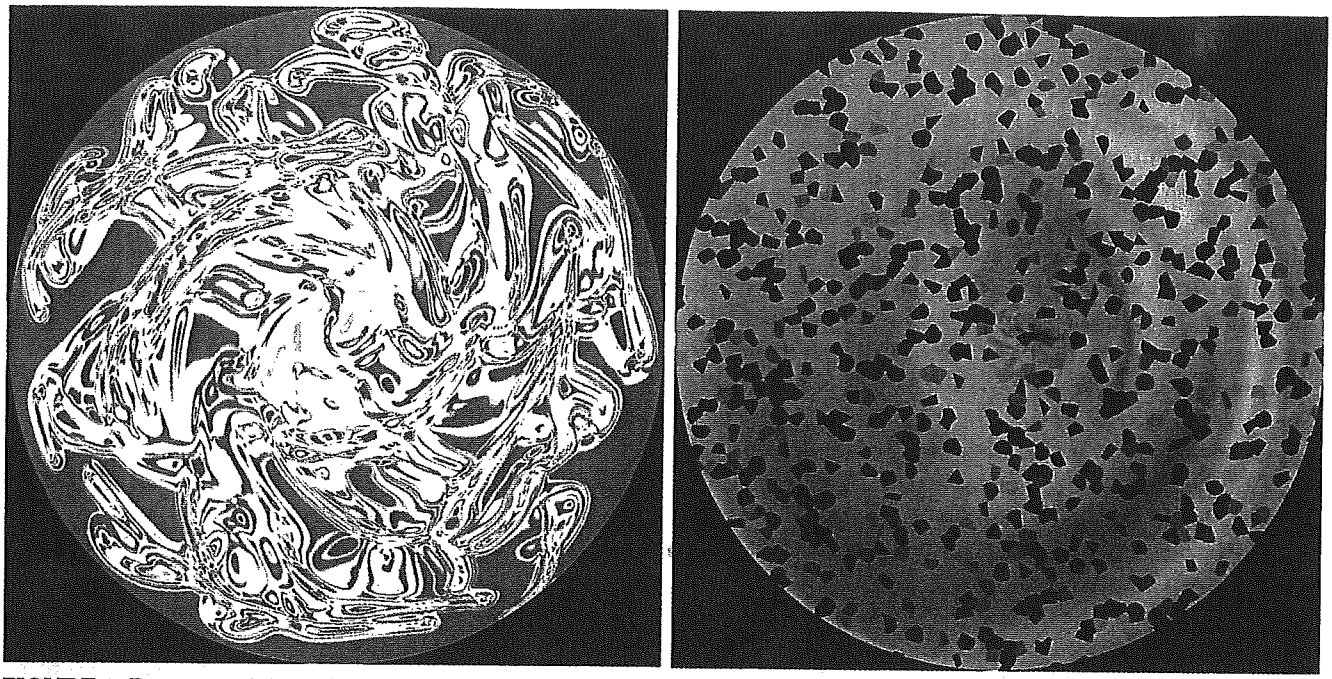

FIGURE 1. Drawings of the early period of vitrectomy made by the patient. (Left panel) The drawing of what the patient saw during early period of vitrectomy. Patient reported seeing colorless swirling fluid. This most likely corresponded to the time of intraocular irrigation of the vitreous cavity during core vitrectomy. (Right panel) The drawing of patient's perceptions at a later time than in the Left panel. Patient reported seeing numerous black and gray spots like snowflakes. This most likely corresponded to the white triamcinolone acetonide crystals being injected intravitreally.

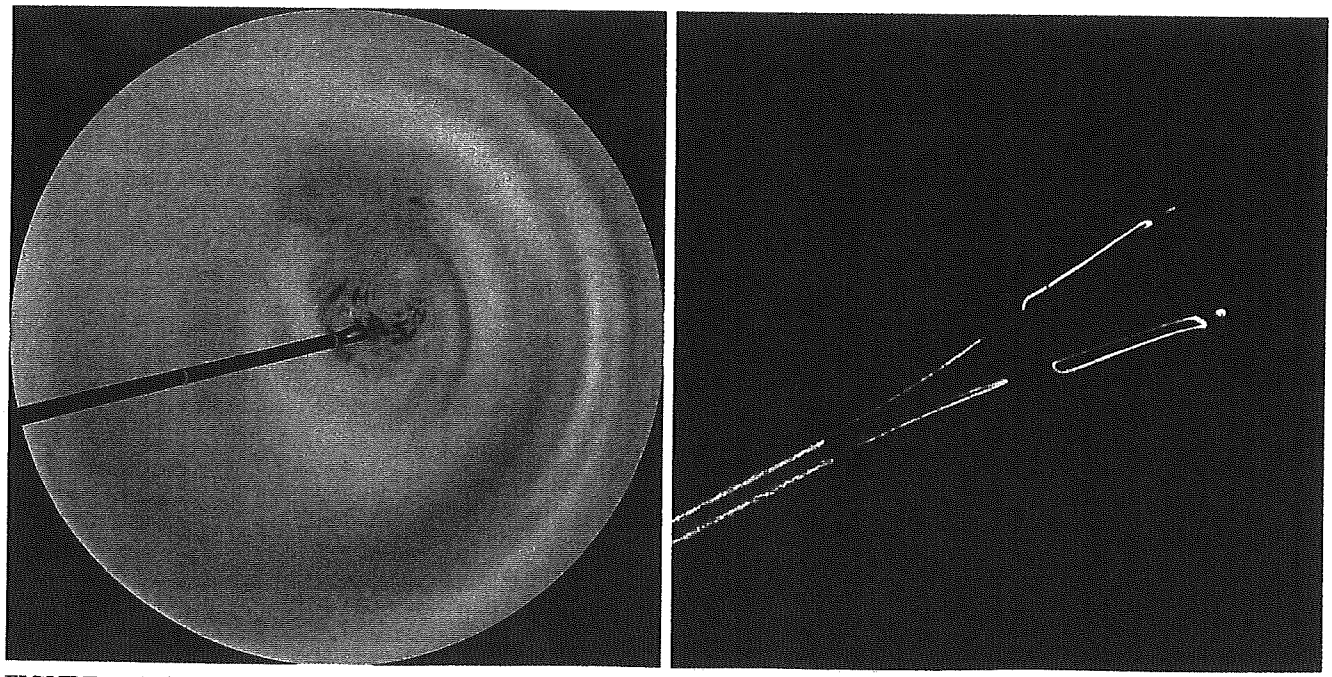

FIGURE 2. A drawing of what the patient saw during membrane peeling and photograph of microforceps. (Left panel) Drawing of what the patient saw just before membrane peeling. Patient reported seeing a sharply tapered instrument coming into the center of the field and peeling off of a membrane-like material. (Right panel) Photograph of the 25-gauge asymmetrical forceps (DORC) used during the surgery. Patient had not seen this instrument before the drawing.

A 56-year-old man with an epiretinal membrane underwent three-port vitrectomy with 25-gauge vitrectomy instruments under retrobulbar anesthesia by 5.0 ml of lidocaine 2%. Following core vitrectomy, triamcinolone acetonide (TA) was injected into the vitreous to improve the visibility of the residual vitreous cortex, and the epiretinal membrane was peeled off with vitreous forceps. Three months later, the patient's visual acuity improved from 20/200 to 20/25.

The patient said that he "enjoyed" the operation because he saw the epiretinal membrane being peeled and understood what was going on. Because he was a professional artist, he was able to draw three different pictures of his visual images during surgery. The patient provided the computer-generated art (Figures 1 and 2 left) on the day after the surgery. For the beginning of surgery, he drew a colorless swirling fluid (Figure 1 left), which probably corresponded to the intraocular irrigation during core vitrectomy. The second picture (Figure 1 right) showed numerous swirling, black and gray spots resembling snowflakes. This image was probably seen when the white TA crystals were injected into the vitreous. The third picture (Figure 2 left) was that of a sharply tapered instrument that moved into the center of the field just before the membrane-like material was peeled off. The color of the instrument was perceived to be silver and black. Strikingly, the patient's drawing was precisely the shape of the tip of the forceps. A photograph of the 25-gauge asymmetrical microforceps (DORC, Zuidland, The Netherlands) used during surgery is shown in Figure 2 right. The shape and color of this instrument was not shown or described to the patient preoperatively. It was confirmed that he had not previously seen the instrument, and that he had made the drawings based only on his recollections from the surgery.

Even though pain is completely relieved by anesthesia, the patient reported seeing objects. It is, however, not explained why an instrument or particles inside the eye can be precisely seen when they are not focused on the retina through the optical system of the eye. We are able to see an entopic image of our retinal blood vessel pattern with transillumination, and the explanation for this is the blocking of the photoreceptors by the blood vessels.[4] Vitreal floaters of a glial ring are similarly explained in cases with a posterior vitreous detachment. The closer the object is to the retina, the smaller and more exact will its shadow be to the actual object. In addition, the patient saw only one instrument on the left-side of his visual field, and the shaft of the light pipe was not seen.

Interestingly, our patient drew a yellow background with some red "hemorrhage-like" pattern. We also had another patient who reported that the intravitreal instrument was silver. Further investigation is needed to elucidate the mechanism of this phenomenon.

REFERENCES

1. Newman DK. Visual experience during phacoemulsification cataract surgery under topical anesthesia. Br J Ophthalmol 2000;84:13–15.
2. Au Eong KG, Lim TH, Lee HM, Yong VS. Subjective visual experience during phacoemulsification and intraocular lens implantation using retrobulbar anesthesia. J Cataract Refract Surg 2000;26:842–846.
3. Au Eong KG, Low CH, Heng WJ, et al. Subjective visual experience during phacoemulsification and intraocular lens implantation under topical anesthesia. Ophthalmology 2000;107:248–250.
4. Westheimer G. Entoptic phenomena. In: Kaufman PL, Alm A, editors. Adler's physiology of the eye. St Louis: Mosby, Inc, 2003:441–452.

Rapid Progression of Diabetic Retinopathy in Eyes With Posterior Uveitis

Judie A. Knol, MD, Bram van Kooij, MD, Harold W. de Valk, MD, PhD, and Aniki Rothova, MD, PhD

PURPOSE: To report on two patients who developed rapid progression of asymmetric diabetic retinopathy (DRP) in eyes affected by posterior uveitis in contrast to their fellow eyes not affected by uveitis.

DESIGN: Observational case report.

METHODS: Two patients with diabetes mellitus (DM) and unilateral uveitis underwent repeated ophthalmologic examinations and fluorescein angiography.

RESULTS: Two patients with DM and unilateral posterior uveitis developed proliferative DRP in eyes with previous uveitis within 3 months after the uveitis subsided. In contrast, the retinal findings of nonuveitic eyes remained unchanged on follow-up of several years.

CONCLUSIONS: Since the pathogenesis of intraocular inflammation and diabetic retinopathy acts through similar biochemical mediators and pathways, it is feasible that posterior uveitis accelerates the progression of diabetic retinopathy. Our results support this hypothesis and point out a risk for rapid retinopathy development in eyes affected with posterior uveitis.

Accepted for publication Sep 6, 2005.

From the Uveitis Center, FC Donders Institute of Ophthalmology (J.A.K., B.v.K., A.R.) and Department of Internal Medicine (H.W.d.V.), University Medical Center Utrecht, Utrecht, The Netherlands.

Inquiries to Aniki Rothova, MD, PhD, FC, Donders Institute of Ophthalmology, University Medical Center, PO Box 85 500, 3508 GA Utrecht, The Netherlands; fax: +31 30 2505 417; e-mail: A.Rothova@oogh.azu.nl

Current Eye Research, 30:813–820, 2005

ISSN: 0271-3683 print / 1460-2202 online
DOI: 10.1080/02713680591006093

Taylor & Francis
Taylor & Francis Group

Toxicity Study of Erucylphosphocholine in a Rat Model

Frank Schuettauf
Department of Ophthalmology,
Eberhard Karls University,
Tübingen, Germany

Kirsten H. Eibl*
Department of Ophthalmology,
Ludwig Maximilians University,
Munich, Germany

Sebastian Thaler and Kei Shinoda
Department of Ophthalmology,
Eberhard Karls University,
Tübingen, Germany

Robert Rejdak
1st Eye Hospital,
Medical University,
Lublin, Poland

C. Albrecht May
Department of Anatomy,
Friedrich Alexander University,
Erlangen, Germany

Georgios Blatsios
Department of Ophthalmology,
Eberhard Karls University,
Tübingen, Germany

Ulrich Welge-Lussen
Department of Ophthalmology,
Ludwig Maximilians University,
Munich, Germany

ABSTRACT *Purpose*: To investigate the effect of intraocular erucylphosphocholine (ErPC) on the retina, the retinal pigment epithelium (RPE), and the choroid in an *in vivo* rat model. *Methods*: Adult male Brown Norway rats were injected intravitreally with ErPC dissolved in balanced salt solution (BSS) at a final concentration of 10 or 100 μM with BSS serving as control. Adverse effects on the anterior and posterior segment were assessed by slit-lamp biomicroscopy and ophthalmoscopy. Retinal toxicity was assessed by electroretinography (ERG), retinal ganglion cell (RGC) quantification, and histology 7 days after intravitreal administration of ErPC. *Results*: There was neither a statistically significant difference in the clinical examination nor in the ERG waves of treated versus control rats 7 days after intravitreal administration of ErPC. Correspondingly, the number of RGC after BSS injection did not differ significantly from ErPC-injected animals. Histologic sections of the posterior segment of 10 and 100 μM ErPC-injected rats did not show any signs of retinal toxicity. Electron microscopy did not display a difference between the 10 μM and the control group. Only the 100 μM-injected animals showed a discrete irregularity of the Müller cell and the retinal ganglion cell cytoplasm at the ultrastructural level. *Conclusions*: ErPC can safely be injected into the vitreous of adult rats at a concentration of 10 μM without any retinal toxicity. Even a 10-fold increase in ErPC concentration leads only to a discrete cytoplasmic irregularity of the innermost retinal layers.

KEYWORDS animal model; electroretinography; intravitreal drug delivery; retinal cells; vitreoretinal pharmacology

INTRODUCTION

Alkylphosphocholines (APCs) represent a new class of pharmacologically active agents with antineoplastic and antiparasitic properties. Due to their good tolerability with only marginal side effects, APCs are in clinical use for the topical treatment of cutaneous breast cancer metastasis (Miltex)[1–3] and for the oral treatment of visceral leishmaniasis (Impavedo).[4,5] Erucylphosphocholine (ErPC), the APC used in this study, is a second-generation APC with an even better pharmacological profile compared to its prototype hexadecylphosphocholine (Miltex; Impavedo). This is due to a simple structural modification, the introduction of a *cis* double bond at the center of the alkyl chain, which is esterified to phosphocholine.[6,7]

Received 14 November 2004
Accepted 6 February 2005

*Kirsten Eibl "contributed equally" with Frank Schuettauf.

Correspondence: PD Dr. med. Ulrich Welge-Luessen, M.D., Department of Ophthalmology, Ludwig Maximilians University, Munich, Mathildenstr. 8, 80336 Munich, Germany.
Fax: ++49-89-5160-3051; E-mail: Ulrich.Welge-Luessen@.med.uni-muenchen.de

In a previous *in vitro* study, we were first to demonstrate that APCs have antiproliferative and anticontractile properties on human retinal pigment epithelial (RPE) cells at nontoxic concentrations.[8] This might be of considerable interest for the treatment of proliferative vitreoretinal diseases like proliferative vitreoretinopathy (PVR).[9–11] As a possible mechanism of action, APCs inhibit protein kinase C function in several cell systems *in vitro*.[8,12–14] Protein kinase C is a membrane-bound G-protein involved in the intracellular cascade of second-messenger systems regulating major cellular functions like proliferation, migration, and contraction.[15]

In ophthalmic research, there are no *in vivo* studies on the use of APCs in the literature so far. After systemic administration in the rat, 20 mg/kg ErPC given at intervals of 48 hr for up to 4 weeks were well tolerated.[16] Although toxicity studies in ophthalmology are mostly performed in the rabbit,[17–19] rat eyes also serve as an established *in vivo* model to investigate the morphological and functional damage caused by the intravitreal application of drugs.[20–24]

Based on our *in vitro* observations on human RPE cells, the purpose of this *in vivo* study was to investigate if an intravitreal administration of ErPC is feasible in the rat and to define a safe concentration interval without toxicity to ocular tissue. To assess possible toxic effects, slit-lamp biomicroscopy, ophthalmoscopy, electroretinography, ganglion cell quantification, and histologic evaluation of the posterior segment were performed 1 week after ErPC injection in the rat eye.

MATERIALS AND METHODS

Alkylphosphocholines

Erucylphosphocholine (ErPC; C22:1-PC; Fig. 1), was synthesized and kindly provided by Prof. Dr. Hansjoerg Eibl (Max Planck Institute for Biophysical Chemistry, Göttingen, Germany). All reagents were of analytical grade as determined by high-performance liquid chromatography. The substance was dissolved in ethanol and stored at 4°C. Independent dilution series in ethanol were used to obtain final concentrations of APCs in equal volumes of ethanol.

Preparation of Solutions

Two erucylphosphocholine (ErPC) solutions with different concentrations were prepared prior to intravitreal injection: 100 μl of a concentration of 10 μM and 100 μM, respectively, in balanced salt solution (BSS, pH 7.4). BSS served as control. The osmolarity of 10 and 100 μM ErPC in BSS corresponds closely to that of BSS only because ErPC is not molecularly dispersed. Due to micelle formation, the number of ErPC particles does not significantly alter the total osmolarity of the BSS solution. The critical micelle concentration (CMC) of ErPC is <0.01 μM.

Intravitreal Injection of ErPC

All experiments were performed in compliance with the guidelines of animal care in the European Community and the Association for Research in Vision and Ophthalmology.

Adult male Brown Norway rats were anesthetized with an intraperitoneal injection of chloral hydrate (6 ml/kg body weight of a 7% solution). Eyes were injected intravitreally using a heat-pulled glass-capillary connected to a microsyringe (Drummond Scientific Co., Broomall, PA, USA) under direct observation through the microscope as described previously.[24] A single injection of 2 μl of 10 or 100 μM ErPC was given. Contralateral eyes served as control eyes and were injected with BSS.

Clinical Examination

To detect possible toxic effects of ErPC to the anterior segment of the eye like corneal opacification and/or cataract induction, eyes were examined by slit-lamp biomicroscopy by an observer unaware of the treatment 0, 1, 24, 48, and 168 hr after the intravitreal injections. Animals with cataract were excluded from the experiment. At the same time points, pupils were dilated with

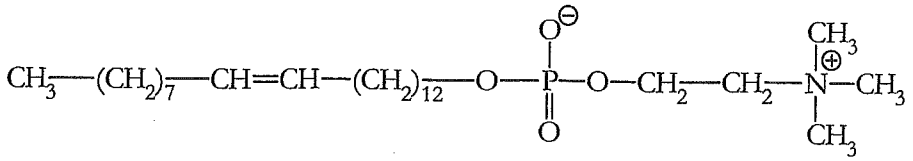

FIGURE 1 Chemical structure of erucylphosphocholine (C22:1-PC).

one drop of a mixture of 1.7% tropicamide and of 3.3% phenylephrine, and indirect ophthalmoscopy was performed to detect vitreous opacification and to verify retinal perfusion.

Electroretinography

Seven days after intraocular injection, each rat from one of the three groups [Group 0, control (BSS); group 1, 10 μM ErPC; group 2, 100 μM ErPC; n = 10, respectively] was kept in a dark room for at least 12 hr and prepared under dim red illumination. Animals were anesthetized with 0.06 ml per kg body weight with 7% chloral hydrate and mounted on a specially designed stereotactic device also containing the electrode mounts (High-Throughput Mouse-ERG, STZ for Biomedical Optics and Function Testing, Tübingen, Germany).[25] Rats were placed on a heating pad throughout the experiment. Pupils were dilated with one drop of a mixture of 1.7% tropicamide and of 3.3% phenylephrine. The ground electrode was a subcutaneous needle in the tail, and the reference electrode was placed subcutaneously between the eyes. The active electrodes were gold wires placed on the cornea with a drop of methylhydroxypropylcellulose (Methocel, Novartis, Basel, Switzerland). Recordings were performed with an ESPION Console (Diagnosys LLC, Littleton, MA, USA). Responses were differentially amplified and filtered by a digital bandpass filter ranging from 0.313 to 1000 Hz to yield a- and b-waves. Oscillatory potentials (OPs) were simultaneously recorded on a different channel with a bandpass filter of 75–300 Hz. Light pulses of 20 cd*s/m^2 and 4-ms duration were delivered via a commercial Ganzfeld stimulator (ESPION ColorBurst Handheld Ganzfeld LED-stimulator, Diagnosys LLC) at a frequency of 0.48 Hz. After recording dark-adapted ERGs, rats were exposed to a white adapting field for 10 min and a light-adapted flicker ERG was recorded to evaluate isolated cone responses. Against a white adapting field (20 cd/m^2), 10 cd*s/m^2 flashes of 4-ms duration were presented at a frequency of 20 Hz. Electrode impedance was checked before and after each measurement in all animals using the machine's built-in feature and was found to be less than 10 kΩ at 50 Hz (manufacturer's recommendation). Responses were stored for offline analysis after averaging 15–20 individual measurements for dark-adapted ERG and 90–100 individual measurements for 20 Hz flicker ERG.

ERG analysis consisted of amplitude and implicit time measurements. The implicit time of the a- and b-waves, the third positive OP peak (OP_3), and the flicker response was measured from stimulus onset to the peak of each wave. The amplitude of the a-wave was measured from baseline to the trough of the a-wave, and the amplitude of the b-wave was determined from the trough of the a-wave to the peak of the b-wave. The amplitude of the OP_3 and the flicker response was measured from preceding negative trough to the peak. Data were analyzed with Student's t test. Differences were considered significant when $p < 0.05$.

Histology

Animals were sacrificed with CO_2 7 days after ErPC or BSS injection. Eyes were enucleated immediately. Following hemisection of the eye along the ora serrata, the cornea, lens, and the vitreous body were removed. Eyecups were immersion-fixed for several days in Ito's solution containing 2.5% glutaraldehyde, 2.5% paraformaldehyde (wt/vol), 0.01% picric acid in 0.1 mol cacodylate buffer (pH 7.2). After rinsing in cacodylate buffer, small sections of the eyecup were postfixed in 1% OSO_4, dehydrated, and embedded in Epon-Araldite in the usual manner. Semithin sections were made from each block using an Ultracut OmU3 microtome (Reichert-Jung) and stained with toluidine blue. Ultrathin sections were stained with uranyl acetate and lead citrate and viewed in a Zeiss electron microscope (EM 902, Zeiss, Oberkochern, Germany).

Quantification of Retinal Ganglion Cells

RGC survival was assessed by retrograde labeling of retinal ganglion cells as described previously.[24] Labeling was performed 5 days after intraocular injection. Animals were anesthetized deeply, and the fluorescent tracer hydroxystilbamidine methanesulfonate (Fluorogold, Molecular Probes, Eugene, OR, USA) was applied to each of the superior colliculi by stereotactic injection as described previously.[26] Two days later, animals were sacrificed by chloral hydrate overdose. After enucleation, the retina was dissected, flat-mounted on cellulose nitrate filters (pore size 60 μm; Sartorius, Long Island, NY, USA), and fixed in 2% PFA for 30 min. Labeled cells were defined as surviving. Observation was performed under a fluorescence microscope immediately, and counting was carried out in 12

distinct areas of 62.500 μm^2 per retina. Images were obtained via a digital imaging system connected to the microscope (ImagePro, Media Cybernetics, Silver Spring, MD, USA), coded, and analyzed semiautomatically in a masked fashion using a computer-assisted image analysis system.

Statistical Analysis

All values are expressed as mean ± SEM. To determine significant differences among groups for RGC counts and for ERG studies, statistical analysis was performed using the paired Student's t test. Differences were considered significant when $p < 0.05$.

RESULTS

Clinical Examination

Rat eyes were injected intravitreally with ErPC without complications. No animal had to be excluded from further analysis due to difficulties of intravitreal drug administration. Also, there was no evidence of toxicity to the anterior segment of the eye like corneal opacification or cataract induction as determined by slit-lamp biomicroscopy. No visible inflammative response like vitreous opacification and/or retinal perfusion defects were recorded at any of the time points as determined by indirect ophthalmoscopy.

Electroretinography

Representative ERG responses are shown in Figure 2. There was no statistically significant difference in the amplitude and implicit time of each ERG component found between 100 μM ErPC–injected eyes and control eyes (BSS). A reduction in amplitude would suggest a reduced number of active cells, whereas a delay in implicit time would reflect a certain impairment of the intraretinal visual transduction pathway. Because the Ganzfeld ERG generates a mass response, a large area of photoreceptor loss must occur before ERG amplitudes display a decrease. However, local tissue damage that might be under the detection limit of a Ganzfeld ERG cannot be completely excluded. From an electrophysiologic point of view, both outer and inner layer functions were well preserved 1 week after intravitreal injection of ErPC at the maximal concentration applied (100 μM).

HISTOLOGY

Sagittal sections through the retina and choroid showed no morphological difference between the control animals and those who received a single intravitreal injection of 10 μM ErPC (Figs. 3A and 3B). The Müller cell processes next to the inner limiting membrane and the ganglion cells with their processes in the nerve fiber layer, both retinal structures to be primarily in contact with the injected ErPC, appeared light- and electronmicroscopically normal. In addition, no changes

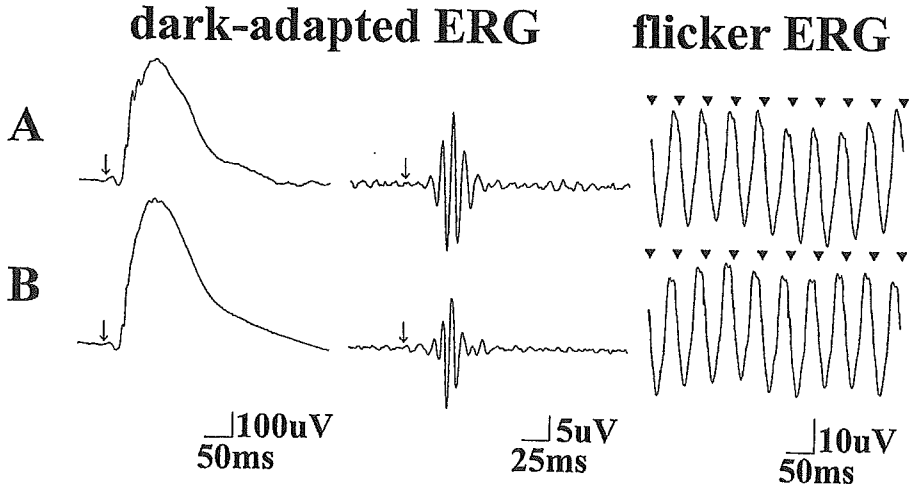

FIGURE 2 Electroretinography (ERG) recorded from a control rat (A) and a rat treated with a single intravitreal injection of 100 μM ErPC (B). A stimulus intensity of 20 cd*s/m^2 was presented to the dark-adapted eyes (dark-adapted ERG), and a stimulus intensity of 10 cd*s/m^2 was superimposed on a background of a stimulus intensity of 20 cd*s/m^2 at light-adapted eyes (flicker ERG). Dark-adapted ERGs were recorded using two different filter settings for a- and b-waves (left column) and oscillatory potentials (OPs) (middle column). Arrow and arrowhead indicate a stimulus onset at 0.48 Hz and 20 Hz, respectively. Note that the scales are different. Statistical comparisons on the amplitude and the implicit time of each component are shown in Table 1.

TABLE 1 Summary of ERG Amplitude and Implicit Time for the Two Groups (Control and 100 μM ErPC; n = 10 in Each Group; See Fig. 2)

		Comparison of each ERG component			
Parameter	Component	Control (BSS)	100 μM ErPC	Unpaired *t* test	p value
Amplitude (μV)	a-wave	-12.0 ± 6.1	-18.8 ± 6.6	n.s.	0.5896
	b-wave	351.2 ± 96.2	358.3 ± 76.5	n.s.	0.8588
	Oscillatory potential (OP_3)	53.2 ± 14.2	55.3 ± 28.8	n.s.	0.8418
	flicker	31.4 ± 10.0	28.2 ± 7.5	n.s.	0.4227
Implicit time (ms)	a-wave	26.1 ± 4.8	25.0 ± 4.0	n.s.	0.5896
	b-wave	96.0 ± 11.2	96.8 ± 8.9	n.s.	0.8720
	Oscillatory potential (OP_3)	48.4 ± 3.8	44.4 ± 6.7	n.s.	0.1308
	flicker	41.8 ± 3.4	40.6 ± 4.0	n.s.	0.4227

Values are presented as mean ± SEM
n.s.; not significant; ERG, electroretinography; ErPC, erucylphosphocholine, BSS, balanced salt solution.

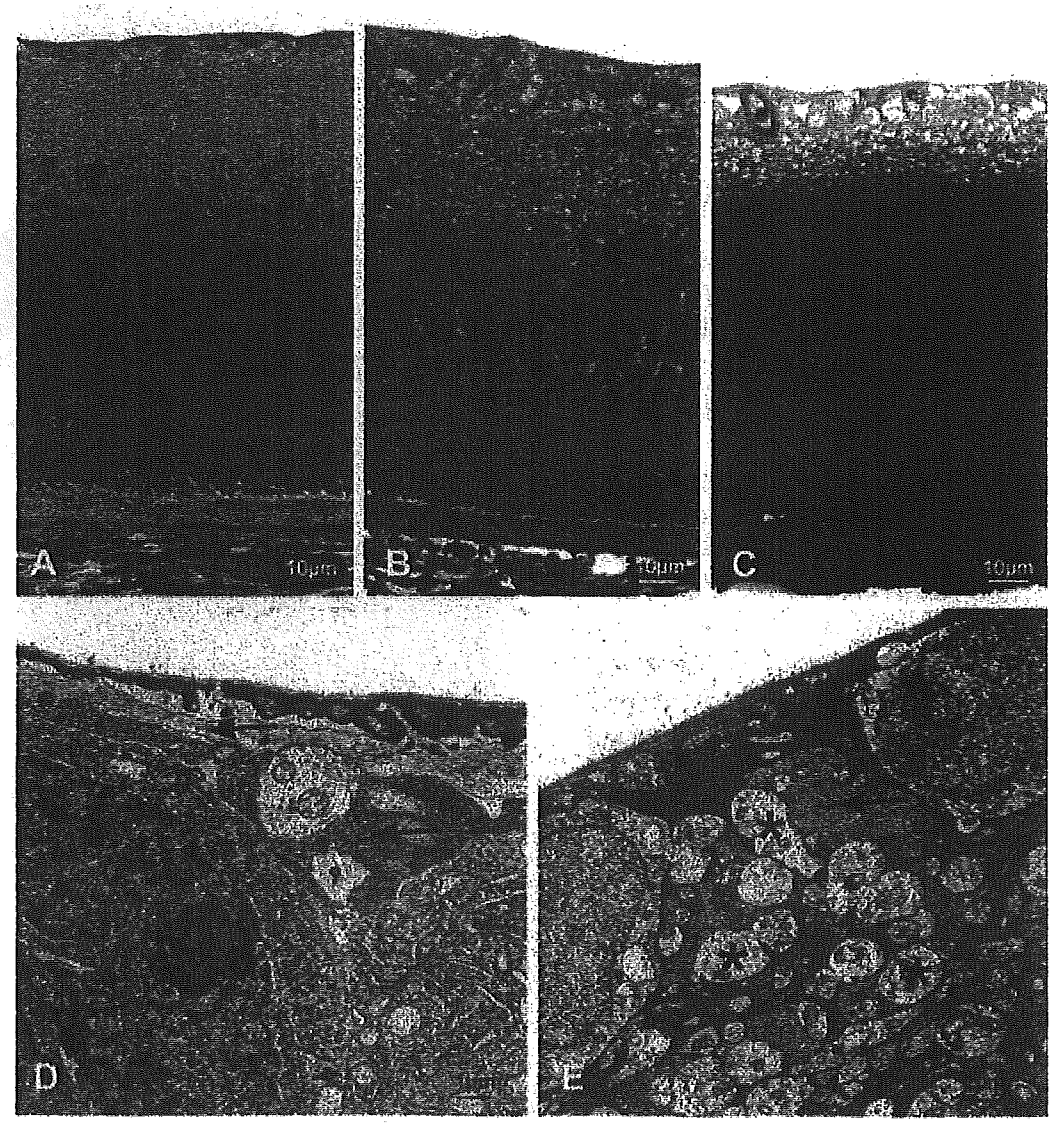

FIGURE 3 Semithin section micrographs of the retina and choroid from a control rat (A) and a rat treated with a single intravitreal injection of 10 μM ErPC (B) and 100 μM ErPC (C). The light-microscopic appearance of all three different retinae is almost identical. (D and E): Electron-microscopic images of the inner retina of an eye treated with 100 μM ErPC. Note the irregularities in the Müller cell processes (arrows) and in the cytoplasm of the ganglion cell processes (asterisks).

were observed in the outer retinal layers and in the choroid.

Eyes treated with 100 μm ErPC revealed some mild morphologically distinctive features. No obvious changes in the inner retina were apparent as determined by light microscopy (Fig. 3C). At the electron microscopic level, the processes of the Müller cells right below the inner limiting membrane were less homogenous in their cytoplasmatic density, showing a few swollen mitochondriae (Fig. 3D). The cytoplasm of the ganglion cells and their processes showed some irregularities in the arrangement of the cell organelles (Fig. 3E). Beside these discrete changes, the outer retina and the choroid of the high-dose-treated eyes appeared normal by both light- and electron microscopic investigation.

Our histological findings indicate a preservation of normal morphology of the eye after intravitreal ErPC injection.

Retinal Ganglion Cell Count

Seven days after intravitreal ErPC administration, the number of RGC did not differ statistically significantly from control eyes (BSS injection). A total of 12 animals was examined in each of the groups [group 0 = control (BSS); group 1 = 10 μM ErPC; group 2 = 100 μM ErPC, respectively].

After administration of 10 μM ErPC (group 1), RGC counts revealed 2145 $\pm$ 226 RGC/mm^2 (mean $\pm$ SEM) 7 days after injection. After intravitreal administration of 100 μM ErPC (group 2), 2177 $\pm$ 202 RGC/mm^2 survived over 7 days ($p = 0.6468$). In BSS-injected eyes, 2125 $\pm$ 332 RGC/mm^2 were counted 7 days after the injection ($p = 0.8637$) (Figs. 4 and 5). The BSS injection itself did not influence RGC survival when compared to untreated eyes (data not shown).

DISCUSSION

To our knowledge, this is the first report on the intravitreal administration of alkylphosphocholines (APCs) in the literature. So far, APCs have been well tolerated when given intravenously, orally, and even topically as an ointment.[3,4,16] Erucylphosphocholine (ErPC) is a second-generation APC and has favorable properties when given intravenously in the rat.[16] This is due to a specific modification in chemical structure,[7] which makes this substance a promising candidate for intravitreal application *in vivo*.

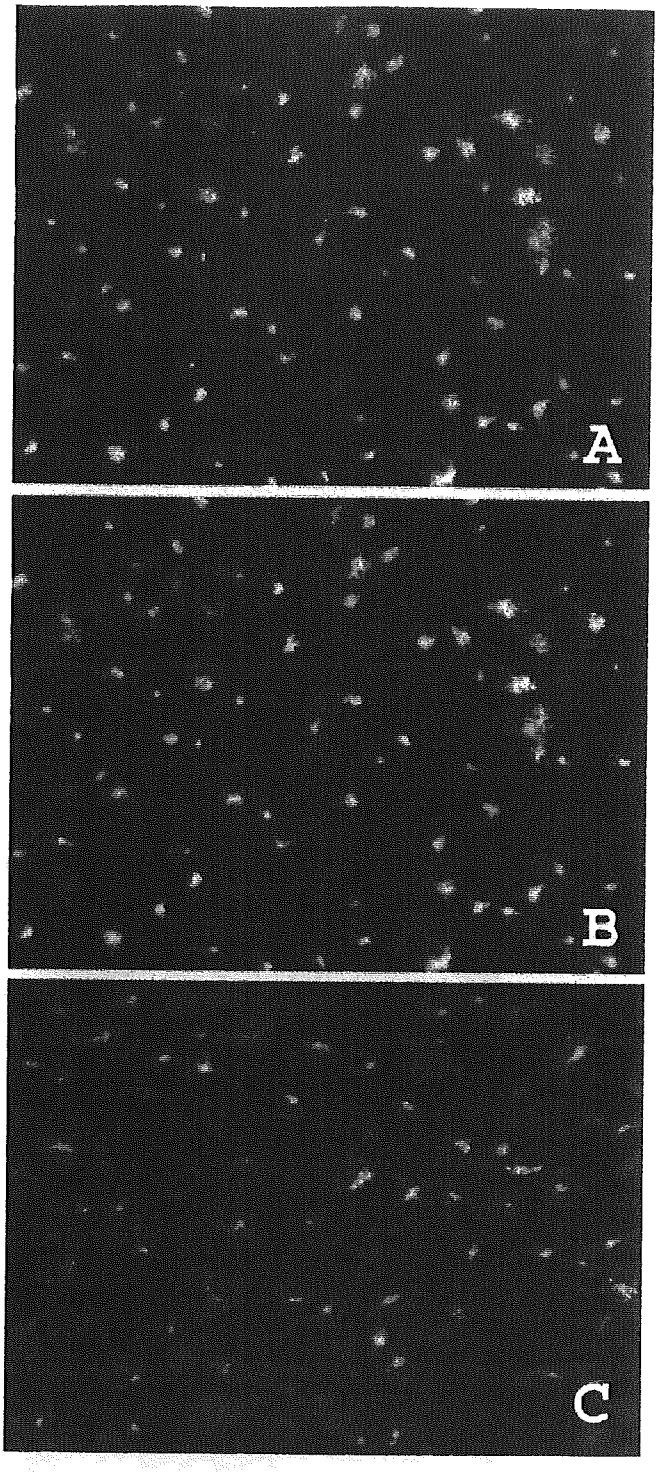

FIGURE 4 Whole mounts of the rat retina 7 days after intraocular injection. Retinal ganglion cells have been back-labeled by the injection of fluorogold. (A) BSS, (B) 10 μM ErPC, (C) 100 μM ErPC.

In ophthalmic research, the rat is a well-established *in vivo* model for the investigation of toxic drug effects.[27–30] Therefore, we chose this animal model to investigate if ErPC has a toxic effect on ocular tissue after intravitreal injection. For this purpose, two different ErPC concentrations were determined based on

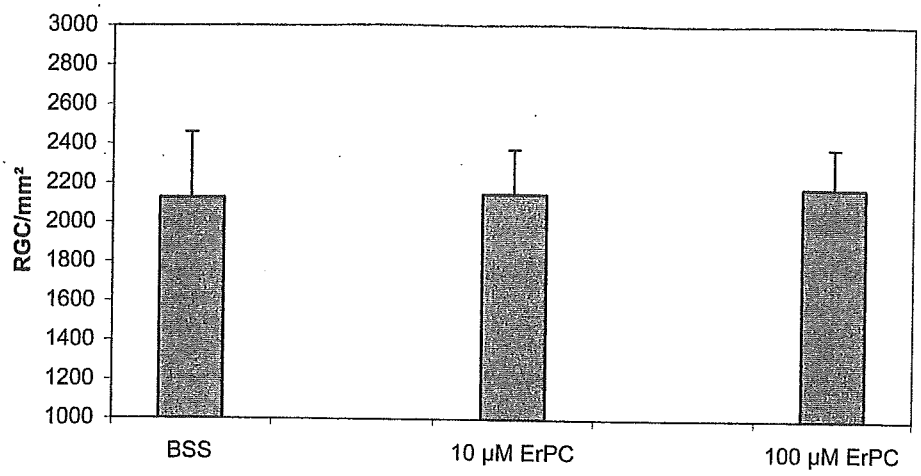

FIGURE 5 RGC survival 7 days after BSS or ErPC injection (10 μM or 100 μM). Values represent the mean ± SEM. No significant difference of RGC survival was observed between the groups.

previous *in vitro* experiments with human retinal pigment epithelial (RPE) cells. In this well-known *in vitro* model for the study of proliferative vitreoretinopathy, ErPC proved to have a good antiproliferative and anticontractile effect without cytotoxicity in the concentration interval examined.[8] These cellular features are crucial for the development of proliferative vitreoretinal diseases such as proliferative vitreoretinopathy.[9,11] As an important pharmacological landmark, the IC_{50} concentration of ErPC was determined to be 10 μM for human RPE cells *in vitro*.[8] The IC_{50} concentration is defined to be the concentration of a substance that inhibits cell proliferation by 50%. We thus chose two different ErPC concentrations for intravitreal administration in the rat and subsequent analysis of ocular toxicity: The IC_{50} concentration of 10 μM and a 10-fold increase in this concentration, 100 μM ErPC. However, the use of data obtained from tissue culture studies to determine the appropriate dose to be applied *in vivo* is difficult. Cultured cells are exposed to a continuous high level of a drug for a long time, whereas the drug level *in vivo* rapidly decreases.

Although we have not observed any toxic effects of ErPC in the rat eye within the concentration interval tested, the results obtained in a rodent model should be handled with care in terms of predictability of possible clinical results. Although the estimated actual concentration of ErPC within the rat vitreous is approximately only a tenth of the concentration injected, the vitreous volume of the rat is rather small compared to larger animals and humans. Thus, the concentrations tested are likely to be safe in other species. Extending these first *in vivo* data to the clinical setting, the effective clinical dose could most probably be even higher.

Regarding drug safety, intravitreal injection in itself bears the risk of an IOP elevation. To avoid an injection-related rise in IOP, the injection volume has been reduced to the minimum possible. Thus, we do not expect an injection-related IOP elevation. As far as ErPC itself is concerned, it is currently unknown if there is any pharmacological effect on the trabecular meshwork and/or the ciliary body. Data from a phase II clinical trial with 23 patients with another alkylphosphocholine, hexadecylphosphocholine (HePC), suggest that there is no effect on IOP in humans 2 and 5 months after systemic administration of HePC.[31] Only reversible effects on the light peak in the electrooculography (EOG) have been observed. In addition, HePC as a first-generation alkylphoshphocholine has significant structural disadvantages compared to ErPC, a second-generation alkylphosphocholine.[6,7] Thus, assumptions made from this compound are limited in their applicability to ErPC.

In this first animal study, we were able to demonstrate the safety of ErPC when administered intravitreally in the rat eye. Now further *in vivo* studies are needed to investigate the efficacy of these new compounds in an animal model of proliferative vitreoretinal disease. In addition, long-term toxicity studies are needed because a sustained drug release system might be advantageous for the prevention of proliferative vitreoretinopathy.

ACKNOWLEDGMENTS

We thank Prof. Dr. Eberhart Zrenner, M.D., and Prof. Dr. Anselm Kampik, M.D., for the careful review of the manuscript and the helpful discussion. We also thank

Anke Fischer for technical assistance with the electron microscopy and Sandra Bernhard-Kurz for the expert technical assistance. This study was supported by grants of the German Research Community (DFG WE 2577/2-1).

REFERENCES

[1] Eibl H, Unger C. Hexadecylphosphocholine: a new and selective antitumor drug. *Cancer Treat Rev.* 1990;17:233–242.

[2] Hilgard P, Engel J. Clinical aspects of miltefosine and its topical formulation Miltex®. *Drugs Today.* 1994;30 (Suppl. B):3–81.

[3] Leonard R, Hardy J, van Tienhoven G, Houston S, Simmonds P, David M, Mansi J. Randomized, double-blind, placebo-controlled, multicenter trial of 6% miltefosine solution, a topical chemotherapy in cutaneous metastases from breast cancer. *J Clin Oncol.* 2001;21:4150–4159.

[4] Kuhlencord A, Maniera T, Eibl H, Unger C. Hexadecylphosphocholine: oral treatment of visceral leishmaniasis in mice. *Antimicrob Agents Chemother.* 1992;36:1630–1634.

[5] Sundar S, Jha TK, Thakur CP, Engel J, Sindermann H, Fischer C, Junge K, Bryceson A, Berman J. Oral miltefosine for Indian visceral leishmaniasis. *N Engl J Med.* 2002;347:1739–1746.

[6] Kötting J, Berger MR, Unger C, Eibl H. Alkylphosphocholines: influence of structural variation on biodistribution at antineoplastically active concentrations. *Cancer Chemother Pharmacol.* 1992;30:105–112.

[7] Sobottka SB, Berger MR, Eibl H. Structure-activity relationships of four anticancer alkylphosphocholine derivatives in vitro and in vivo. *Int J Cancer.* 1993;53:418–425.

[8] Eibl KH, Banas B, Schoenfeld CL, Neubauer AS, Priglinger S, Kampik A, Welge-Luessen U. Alkylphosphocholines inhibit proliferation of human retinal pigment epithelium. *Invest Ophthalmol Vis Sci.* 2003;44:3556–3561.

[9] Hiscott PS, Grierson I, McLeod D. Retinal pigment epithelial cells in epiretinal membranes: an immunohistochemical study. *Br J Ophthalmol.* 1984;68:708–715.

[10] Hiscott P, Sheridan C, Magee RM, Grierson I. Matrix and the retinal pigment epithelium in proliferative retinal disease. *Prog Retin Eye Res.* 1999;18:167–190.

[11] Asaria RHY, Kon CH, Bunce C, Charteris DG, Wong D, Khaw PT, Aylward GW. Adjuvant 5-fluouracil and heparin prevents proliferative vitreoretinopathy. *Ophthalmology.* 2001;108:1179–1183.

[12] Zheng B, Oishi K, Shoji M, Eibl H, Berdel WE, Hajdu J, Vogler WR, Kuo JF. Inhibition of protein kinase C, (sodium plus potassium)-activated adenosine triphosphatase, and sodium pump by synthetic phospholipid analogues. *Cancer Res.* 1990;50:3025–3031.

[13] Shoji M, Raynor RL, Fleer EAM, Eibl H, Vogler WR, Kuo JF. Effects of hexadecylphosphocholine on protein kinase C and TPA-induced differentiation of HL60 cells. *Lipids* 1991;26:145–149.

[14] Überall F, Oberhuber H, Maly K, Zaknun J, Demuth L, Grunicke HH. Hexadecylphosphocholine inhibits inositol phosphate formation and protein kinase C activity. *Cancer Res.* 1991;51:807–812.

[15] Nishizuka Y. Intracellular signalling by hydrolysis of phospholipids and activation of protein kinase C. *Science.* 1992;258:607–614.

[16] Erdlenbruch B, Jendrossek V, Gerriets A, Vetterlein F, Eibl H, Lakomek M. Erucylphosphocholine: pharmacokinetics, biodistribution and CNS-accumulation in the rat after intravenous administration. *Cancer Chemother Pharmacol.* 1999;44:484–490.

[17] Cannon JP, Fiscella R, Pattharachayakul S, Garey KW, De Alba F, Piscitelli S, Edward DP, Danziger LH. Comparative toxicity and concentrations of intravitreal amphotericin B formulations in a rabbit model. *Invest Ophthalmol Vis Sci.* 2003;44:2112–2117.

[18] Maia M, Margalit E, Lakhanpal R, Tso MO, Grebe R, Torres G, Eong KG, Farah ME, Fujii GY, Weiland J, *et al.* Effects of intravitreal indocyanine green injection in rabbits. *Retina.* 2004;24:69–79.

[19] Rowley SA, Vijayasekaran S, Yu PK, McAllister IL, Yu DY. Retinal toxicity of intravitreal tenecteplase in the rabbit. *Br J Ophthalmol.* 2004;88:573–578.

[20] Sun Q, Ooi VE, Chan SO. N-methyl-D-aspartate-induced excitotoxicity in adult rat retina is antagonized by single systemic injection of MK-801. *Exp Brain Res.* 2001;138:37–45.

[21] Macky TA, Oelkers C, Rix U, Heredia ML, Kunzel E, Wimberly M, Rohrer B, Crosson CE, Rohr J. Synthesis, pharmacokinetics, efficacy, and rat retinal toxicity of y novel mitomycin C-triamcinolone acetonide conjugate. *J Med Chem.* 2002;45:1122–1127.

[22] Enaida H, Sakamoto T, Hisatomi T, Goto Y, Ishibashi T. Morphological and functional damage of the retina caused by intravitreous indocyanine in rat eyes. *Graefes Arch Clin Exp Ophthalmol.* 2002;240:209–213.

[23] Chidlow G, Osborne NN. Rat retinal ganglion cell loss caused by kainate, NMDA and ischemia correlated with a reduction in mRNA and protein of Thy-1 and neurofilament light. *Brain Res.* 2003;963:298–306.

[24] Rejdak R, Zarnowski T, Turski WA, Kocki T, Zagorski Z, Zrenner E, Schuettauf F. Alterations of kynurenic acid content in the retina in response to retinal ganglion cell damage. *Vision Res.* 2003;43:497–503.

[25] Dalke C, Löster J, Fuchs H, Gailus-Durner V, Soewarto D, Favor J, Neuhäuser-Klaus A, Pretsch W, Gekeler F, Shinoda K, *et al.* Electroretinography as a screening method for mutations causing retinal dysfunction in mice. *Invest Ophthalmol Vis Sci.* 2004;45:601–609.

[26] Schuettauf F, Naskar R, Vorwerk CK, Zurakowski D, Dreyer EB. Ganglion cell loss after optic nerve crush mediated through AMPA-Kainate and NMDA receptors. *Invest Ophthalmol Vis Sci.* 2000;41:4313–4316.

[27] Seme MT, Summerfelt P, Neitz J, Eells JT, Henry MM. Differential recovery of retinal function after mitochondrial inhibition by methanol intoxication. *Invest Ophthalmol Vis Sci.* 2001;42:834–841.

[28] Goto W, Ota T, Morikawa N, Otori Y, Hara H, Kawazu K, Miyawaki N, Tano Y. Protective effects of timolol against the neuronal damage induced by glutamate and ischemia in the rat retina. *Brain Res.* 2002;958:10–19.

[29] Yoneda S, Tanaka E, Goto W, Ota T, Hara H. Topiramate reduces excitotoxic and ischemic injury in the rat retina. *Brain Res.* 2003;967:257–266.

[30] Goto Y, Taniwaki T, Shigematsu J, Tobimatsu S. The long-term effects of antiepileptic drugs on the visual system in rats: electrophysiological and histopathological studies. *Clinic Neurophysiol.* 2003;114:1395–1402.

[31] Theischen M, Bornfeld N, Becher R, Keller U, Wessing A. Hexadecylphosphocholine may produce reversible functional defects of the retinal pigment epithelium. *Ger J Ophthalmol.* 1993;2:113–115.

tapraid3/zrx-ajopht/zrx-ajopht/zrx00806/zrx5377d06z | xppws | S=1 | 2/27/06 | 19:07 | Art: 5377 | DTD5.0

Expression of VEGF and PEDF in Choroidal Neovascular Membranes Following Verteporfin Photodynamic Therapy

AQ: 1

AQ: 2 OLCAY TATAR, MD, ANNEMARIE ADAM, KEI SHINODA, MD, PHD, PETER STALMANS, MD, PHD, CLAUS ECKARDT, MD, MATTHIAS LÜKE, MD, KARL ULRICH BARTZ-SCHMIDT, MD, AND SALVATORE GRISANTI, MD

• PURPOSE: To examine the impact of photodynamic therapy (PDT) on pigment epithelium derived factor (PEDF) expression in human choroidal neovascularization (CNV) membranes with regard to vascular endothelial growth factor (VEGF) expression.

• DESIGN: Interventional case series.

• METHODS: Retrospective review of interventional case series of 42 patients (42 eyes) who underwent removal of CNV. CNV was secondary to age-related macular degeneration in all cases. Fifteen patients were treated with PDT, 3 to 246 days before surgery. CNV were stained for CD34, CD105, cytokeratin 18, VEGF, and PEDF. Twenty-seven CNV without previous treatment were used as control.

• RESULTS: Specimens without pretreatment disclosed varying degrees of vascularization, VEGF, and PEDF expression by different cells. Specimens treated by PDT, 3 days previously showed mostly occluded vessels lined with damaged endothelial cells (EC). In contrast, specimens excised at later time points after PDT were highly vascularized with healthy EC. This chronology was associated with an impressive VEGF immunoreactivity AQ: 4 increased considerably in retinal pigment epithelial cells as well as significantly reduced PEDF expression in EC and stroma.

• CONCLUSIONS: PDT induces a selective vascular damage in CNV. The effectiveness of PDT, however, seem to be jeopardized by a rebound effect initiated by an enhanced VEGF and reduced PEDF expression in CNV. (Am J Ophthalmol 2006;xx:xxx. © 2006 by Elsevier Inc. All rights reserved.)

Accepted for publication Jan 27, 2006.

From the Department of Ophthalmology, Eberhard-Karls University, Tuebingen, Germany (O.T., M.L., K.U.B.-S., S.G.); Department of Pathology, Eberhard-Karls University, Tuebingen, Germany (A.A.); Laboratory of Visual Physiology, National Institute of Sensory Organs, Tokyo, Japan (K.S.); Department of Ophthalmology, UZ St.-Rafael, Leuven, Belgium (P.S.); and Augenklinik der Stadtischen Kliniken, Frankfurt am Main, Germany (C.E.).

Supported by the Jung Foundation, the Grimmke Foundation, and the AQ: 3 Vision 100 Foundation.

Inquiries to Salvatore Grisanti, MD, Department of Ophthalmology, Division of Vitreoretinal Surgery, Eberhard-Karls University Tuebingen, Schleichstrasse 12-15, 72076 Tuebingen, Germany; e-mail: Salvatore.Grisanti@med.uni-tuebingen.de

AGE-RELATED MACULAR DEGENERATION (AMD) IS the leading cause of legal blindness in patients older than 60 years of age in the western world.[1] Neovascular AMD with the development of choroidal neovascularization (CNV) in the macular area accounts for 80% of the severe loss of visual acuity attributable to AMD.[2,3] Numerous treatment modes have been attempted to destroy the pathologic blood vessels using thermal photocoagulation, ionizing radiation or photosensitizing dyes, or to surgically remove the neovascular tissue with or without replacement of the damaged retinal pigment epithelium or translocation of the fovea. AQ: 5

PDT with verteporfin (Visudyne, Novartis AG, Buelach, Switzerland) is an effective treatment for subfoveal choroidal neovascularization secondary to AMD and is accepted as a routine procedure under certain circumstances.[4–8] PDT is based on the targeted photoactivation of the intravenously given photosensitive drug. The activated dye results in the creation of oxygen intermediates and free radicals affecting the exposed endothelial cells (EC).[9] PDT allows selective photothrombosis of the CNV. However, a recurrence rate of approximately 90% within 3 months and a mean visual loss of 2 ETDRS lines within 6 months, limit its effectiveness.[4–6]

Although submacular removal of the CNV is not favored by the recently published results of submacular surgery trials,[10] both macular translocation of the retina as well as autologous retinal pigment epithelium and choroid transplantation are the advanced surgical treatment options.[11,12] According to the small case series, surgical treatment still remains an option for those who do not benefit enough from prior PDT[13,14] (Johnson MW, ARVO Meeting, 2005, Abstract).

0002-9394/06/$32.00
doi:10.1016/j.ajo.2006.01.085

TABLE. Clinical Characteristics of the Patients Treated with PDT Before Surgical Removal of the CNV

Patient	Eye	Age/Gender	CNVM Type	Visual Acuity	PDT Treatments	Time to Surgery From the First PDT/Last PDT
1	L	76/m	classic	0.025	1	3 days
2	R	78/f	classic	0.02	1	3 days
3	L	54/m	predom. classic	0.063	2	113/3 days
4	L	84/m	classic	0.025	1	3 days
5	L	83/m	classic	0.03	1	34 days
6	L	85/f	classic	1/35 MV	1	37
7	R	73/f	occult	0.1	3	208/138/40 days
8	L	79/m	Pred. classic with hemorrhagy	0.1	1	55 days
9	R	80/f	classic	0.1	2	172/69 days
10	L	77/m	min. classic with RAP	0.6	1	84 days
11	L	76/f	occult (peripapillary)	0.6	1	105 days
12	L	81/m	occult	0.08	2	213/131 days
13	R	70/f	min. classic	0.05	2	151/132 days
14	L	78/f	classic	0.05	3	344/222/146 days
15	R	74/f	hemorrhagic	0.3	1	246 days

CNV = choroidal neovascularization; PDT = photodynamic therapy; MV = meter vision; f = female; m = male; min. = minimally; predom. = predominantly; RAP = retinal angiomatous proliferation.

New antiangiogenic treatment modalities applied either alone or in combination with PDT seem to be a great advance in neovascular AMD treatment.[15-17] However, the understanding of the high rate of recurrences after PDT as well as impacts of PDT on angiogenesis in human CNV is, unfortunately, limited. Herein, we present our results of the clinicopathological evaluation of those cases treated with verteporfin PDT before the surgery. Our analysis focuses on the angiogenesis stimulatory and inhibitory factors, namely vascular endothelial growth factor (VEGF) and pigment epithelium derived factor (PEDF), respectively, expressed within the specimens extracted after different time intervals and numbers of PDT treatments.

METHODS

• SUBJECTS AND TREATMENTS: We retrospectively reviewed 42 eyes of 42 consecutive AMD patients, in which surgery for CNV was performed. In 15 of these patients, surgery was performed after verteporfin PDT (Table). In addition to the complete ophthalmologic examination, in patients receiving verteporfin PDT, stereoscopic fluorescein angiography (FA) was performed before the treatment and perioperatively. CNV was classified according to the guidelines of the TAP and VIP studies.[4-8] Therapy options, including observation, conventional thermal laser photocoagulation, PDT retreatment, macular translocation with 360 degrees retinotomy, and CNV membrane extraction were discussed with the patients. Surgical intervention was considered when (1) visual acuity was below 20/200 being the minimum visual acuity to recommend the first PDT according to the TAP-investigation,[4,5] (2) visual deterioration progressed after initial PDT, (3) patient refused retreatment with PDT because of continuous visual deterioration in the fellow eye despite PDT, and (4) retreatment with PDT was impossible due to recurrent or massive submacular hemorrhage. Clinical characteristics of the patients treated with verteporfin-PDT are summarized in the Table. Each patient gave written informed consent after the experimental nature of the treatment procedure, and the risks and benefits of all therapeutic options were discussed in details. The study followed the guidelines of the declaration of Helsinki as revised in Tokyo and Venice. The study and the histologic analysis of the specimens were approved by the local Institutional Review Board.

Four eyes underwent CNV extraction 3 days after PDT. Three of these four eyes had subfoveal classic CNV. The visual acuity of these three eyes was between 4/200 and 10/200, less than the 20/200 that was the lowest permissible visual acuity for PDT in the TAP-investigation.[4,5] The fourth patient had predominantly classic CNV and experienced decrease in visual acuity from 60/200 to 10/160 accompanied by leakage in FA, 3 months after the first PDT. He opted to proceed with macular surgery instead of PDT retreatment. PDT 3 days before surgery was intended to reduce the risk of bleeding at the time of surgical extraction.

• TISSUE PREPARATION AND IMMUNOHISTOLOGY: Within minutes after surgery, excised CNV membranes were fixed in formalin 3.7% and embedded in paraffin. After serial sections were deparaffinized and rehydrated, antigen retrieval was accomplished by proteolytic digestion with

AQ: 11 pronase 0.5% (Sigma, St Louis, Missouri, USA) for PEDF and cytokeratin18 (CK18) and with proteinase K (Dako) for VEGF.

Immunohistochemical staining for CD34 (Mouse, Mab, Immunotech, Hamburg, FRG), CD105 (Mouse, Mab, Clone AQ: 12 SN6 hours, Dako), and CK18 (Mouse, Mab, Progen, Heidelberg, Germany) was performed using the horseradish peroxidase method as we have described previously.[18] The brown chromogen diaminobenzidine was used for CD34 and CD105 but AEC high sensitive substrate red chromogen (Cytomation, Code K3461, Dako) for CK18 staining.

Immunohistochemical staining for VEGF and PEDF were performed by the alkaline-phosphatase method according to the manufacturer's instructions (ChemMate Detection Kit, Alkaline Phosphatase/RED, Rabbit/Mouse, K5005; Dako). A monoclonal mouse antihuman VEGF antibody specific for VEGF-A (clone C-1; Santa Cruz Biotechnology, Santa Cruz, California, USA) and a monoclonal mouse antihuman PEDF antibody (MAB 1059; AQ: 13 Chemicon International, California, USA) were used. The biotinylated goat antimouse secondary antibody was followed by Streptavidin conjugated to alkaline phosphatase and chromogen red. Levamisole was applied to inhibit endogenous alkaline phosphatase activity. Hematoxylin III according to Gill (Merck, Darmstadt, Germany) was used as a counterstain. For negative controls, the primary antibodies were substituted by appropriate normal sera or omitted.

• ANALYSIS: Serial sections from a specimen were analyzed independently by two masked observers (O.T., S.G.) by light microscopy.

Vascularization was calculated by counting the number of AQ: 14 CD34 and CD105 positive vascular-like patterns in the most vascularized area under ×200 magnification. CNV membranes were classified semiquantitatively as "hypocellular" when cellular infiltration within the stroma was more dominant than fibrosis or "hypercellular" when fibrosis was dominant with minor cellular infiltration.

Immunoreactivity for VEGF and PEDF were analyzed separately in retinal pigment epithelium, EC, and stroma. A grading scheme indicating the degree was used: 3, 2, 1, and 0 were assigned to indicate intense (70% to 100% positive cells); moderate (40% to 69% positive cells); weak VEGF labeling (1% to 39% positive cells), and absence of any staining, respectively.

Predominance score of VEGF to PEDF (PS) is defined for retinal pigment epithelium, EC, and stroma of each membrane calculating the difference between VEGF and PEDF staining scores in each component. The intensity of VEGF and PEDF immunostainings as well as "the predominance score of VEGF to PEDF" between the defined subgroups were analyzed with Mann-Whitney U test. $P \leq .05$ was considered significant.

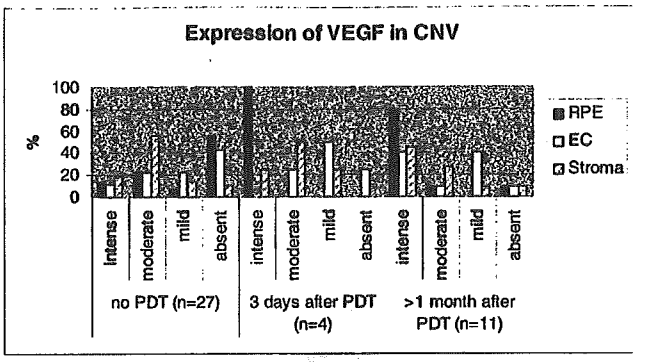

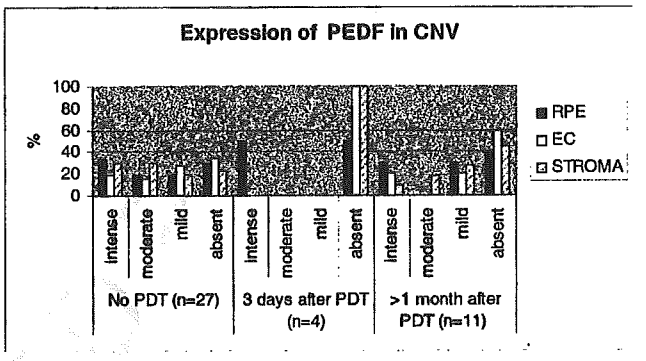

FIGURE 1. Graphs showing "vascular endothelial growth factor" (VEGF) (Top) and "pigment epithelium derived factor" (PEDF) (Bottom) in choroidal neovascularization (CNV) without pretreatment or extracted 3 days and longer than 1 month after photodynamic therapy (PDT). VEGF and PEDF immunostaining in retinal pigment epithelium (RPE,), endothelial AQ: 26 cells (EC,) and stromal cells () were evaluated separately and AQ: 27, AQ: 28 semiquantitatively as intense, moderate, mild or absent.

RESULTS

• ANGIOGRAPHIC CLASSIFICATION AND CHARACTERIZATION: The angiographic features differed depending on the post-PDT time interval (Table). In all of the four membranes extracted 3 days after PDT, a hypofluorescence suggesting nonperfusion of the irradiated area and the CNV was seen in early phases of angiography at the day of surgery. Late phases of FA revealed hyperfluorescence and leakage at the fovea consistent with choroidal ischemia. In CNV membranes extracted at longer post-PDT intervals, FA on the day of surgery disclosed membranes with leakage in late phases (data not shown).

• IMMUNOHISTOPATHOLOGIC FINDINGS: Gradings of immunoreactivity of VEGF and PEDF in untreated and PDT treated CNV groups are summarized in Figure 1, Top F1 and Bottom, respectively.

• HISTOPATHOLOGICAL FINDINGS IN CNV WITHOUT PDT: All but one membrane was vascularized as evidenced by CD 34 positive vessels. All vessels were

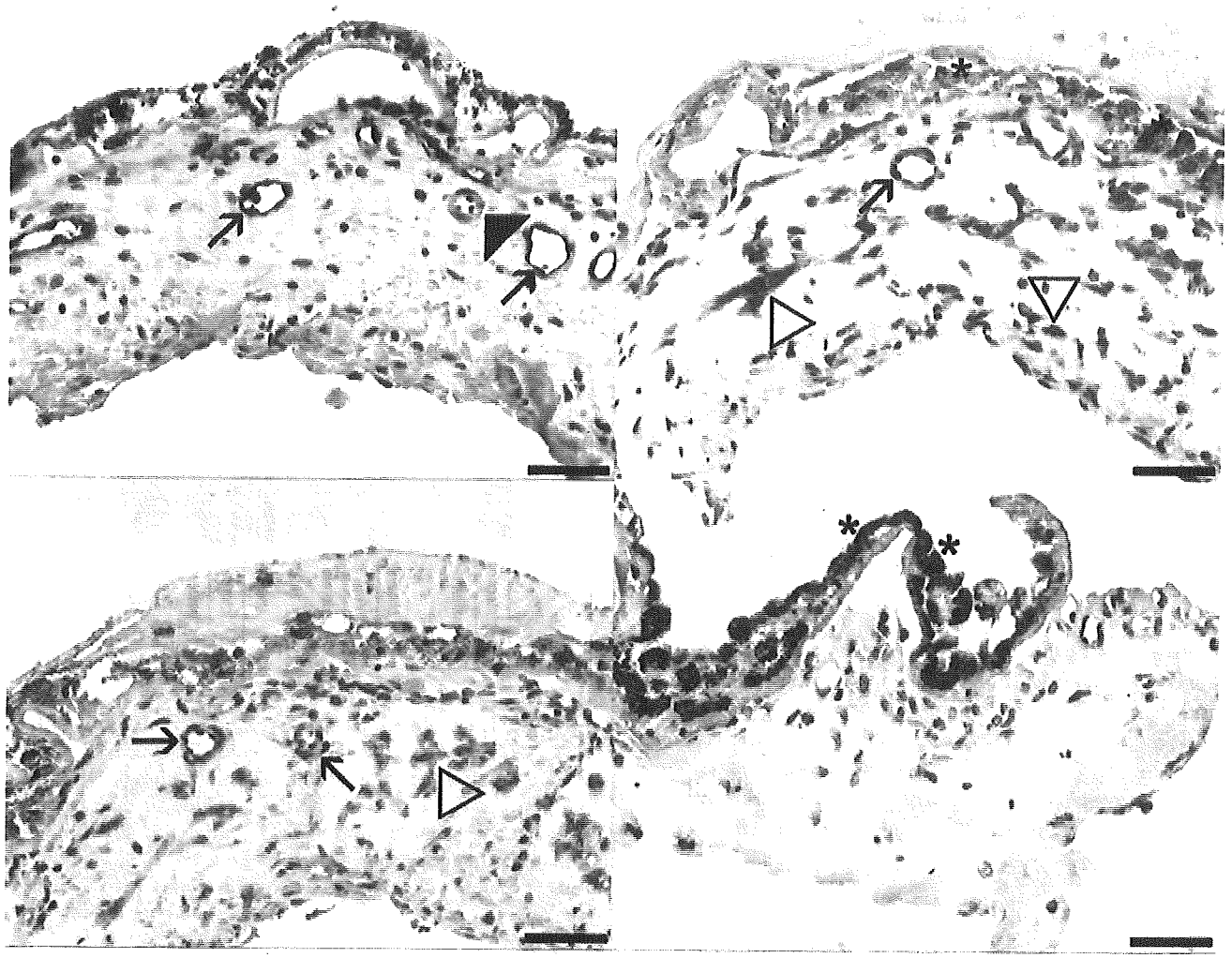

FIGURE 2. Photomicrographs of two surgically excised CNV without prior PDT. The specimens were probed with antibody against CD 105 (Top left), stained with 3-Diaminobenzidine resulting in a brown chromogen, and (Top right) VEGF and (Bottom left and right) PEDF stained with red chromogen. Hematoxylin was used as counterstain. Both membranes disclose a retinal pigment epithelium cell layer (asterisk), vascularization (arrows), fibroblastic stroma cells, and different degrees of an inflammatory infiltration (white arrow head). The activated endothelial cell marker CD105 is selectively expressed in vascular structures (for example, arrows), however, some endothelial cells do not stain for CD105 (arrow head). The brown chromogen can be distinguished from the melanin granula (asterisk) contained in pigmented cells (Top left). In the serial section of the same specimen (Top right), VEGF staining can be detected within endothelial cells (arrow) and stromal cells (white arrow head), whereas retinal pigment epithelium cells are negative or very faintly stained (asterisk). In another serial section probed with PEDF (Bottom left), stromal cells (inflammatory cells and fibroblasts) (white arrow head) and endothelial cells (arrows) are shown to express PEDF. In a distinct specimen (Bottom right), retinal pigment epithelium cells with strong PEDF staining are detected (asterisk). Scale bars: 50 μm.

stained positively for CD 34 but only partially for CD105 (Figure 2, Top left). Of the specimens, 40.7% (11 of 27) were hypocellular. Retinal pigment epithelium cells immunoreactive for CK18 were found in all specimens.

VEGF staining was absent in the retinal pigment epithelium cells of 65.6% (15 of 27) of the specimens. In only four of the specimens (14.8%), VEGF staining was strong. EC expressed VEGF in 55% (15 of 27) of the specimens whereas staining intensity was strong only in 14.8% (4 of 27) of them. Within the stroma, VEGF appeared to be present both in fibroblast like and inflammatory cells in 93.3% of the specimens. (Figure 1, Top, Figure 2, Top right).

Contrary to VEGF, PEDF was expressed in retinal pigment epithelium cells of 70% (19 of 27) of the specimens, mostly in strong and moderate intensities but weak only in 15.8% (4 of 27) of the samples. PEDF expression was found in vascular EC and stromal cells like fibroblasts in 63% (17 of 27) and 78% (21/27) of the membranes, respectively. (Figure 1, Bottom, Figure 2, Bottom left and right).

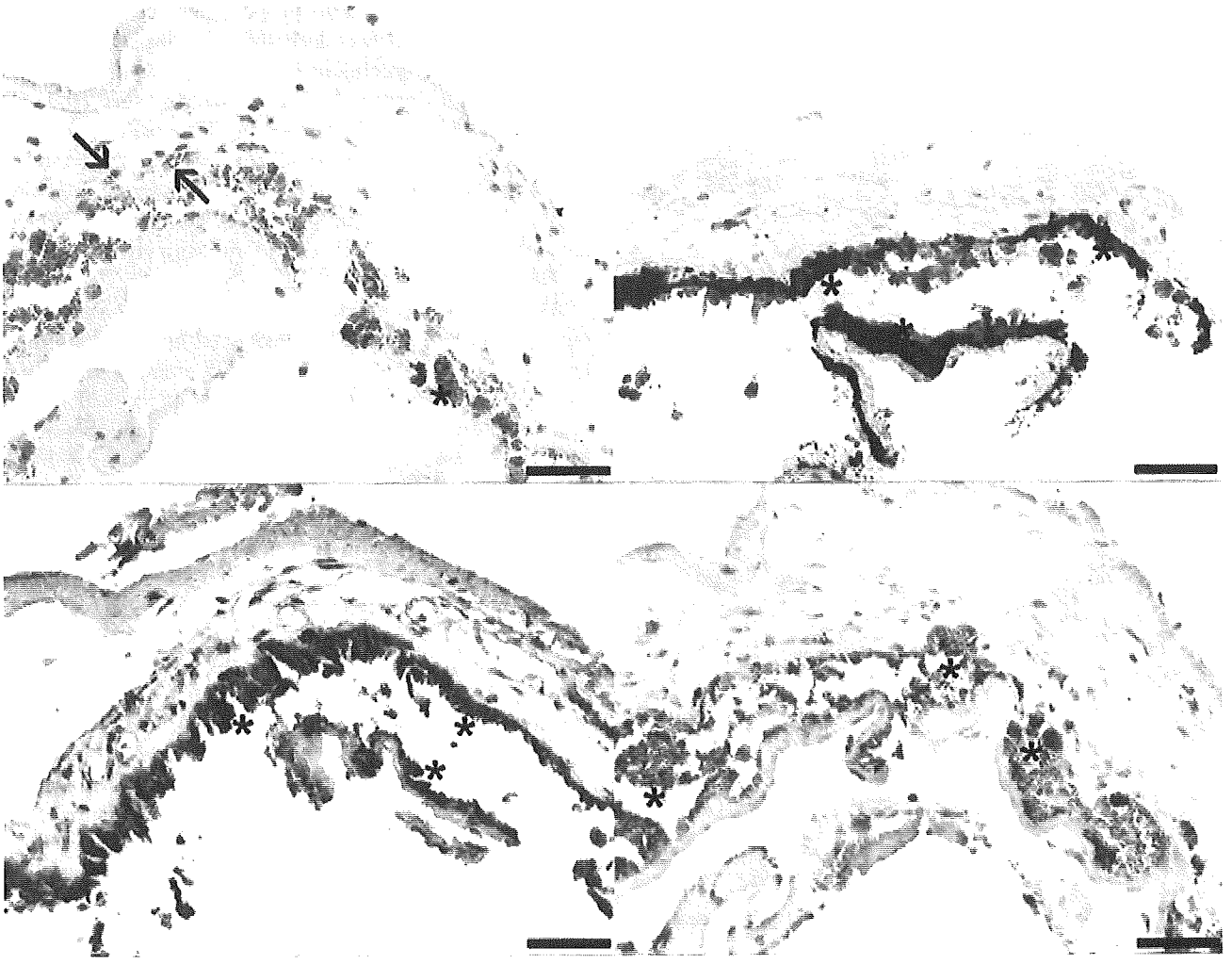

COLOR

FIGURE 3. Photomicrographs of CNV membrane (patient 2 in Table), extracted 3 days after PDT. The serial sections were probed with CD105 (Top left), Cytokeratin 18 (Top right), VEGF (Bottom left), and PEDF (Bottom right). Most of the vessels depicted by the brown chromogen are collapsed and lined with damaged endothelial cells (arrows). Retinal pigment epithelium cells (Top right; asterisk) are strong positive for VEGF (Bottom left, asterisk) but do not display PEDF (Bottom right, asterisk). Scale bars: 50 μm.

• HISTOPATHOLOGICAL FINDINGS IN CNV 3 DAYS AFTER PDT TREATMENT: In membranes extracted 3 days after PDT (n = 4), immunohistology with CD34 and CD105, disclosed mostly collapsed vessels. Morphologically, the EC lining the parent vessels appeared severely damaged (Figure 3, Top left). All specimens were hypocellular.

In all these four membranes, CK18 positive retinal pigment epithelium cells (Figure 3, Top right) displayed an intense staining for VEGF (Figure 3, Bottom left) that is significantly increased in comparison to the control group (P = .0035). PEDF expression was strongly positive in retinal pigment epithelium cells of the two membranes whereas the other two specimens did not disclose any PEDF at all. Predominance score of VEGF to PEDF in retinal pigment epithelium of these membranes were significantly higher than that in the control group (PS = 1.5, PS = −1, respectively, P = .0299).

Only one membrane disclosed moderate expression of VEGF in EC. EC in the other three specimens were either negative (n = 1) or just weakly (n = 2) stained (Figure 1, Top). VEGF expression in stroma varied between weak and strong intensity. Contrary to the control group, none of these four specimens displayed PEDF either in EC or stroma and decrease in PEDF expression in EC and stroma was significant. (P = .0286, .0102, respectively) (Figure 1, Bottom, Figure 3, Bottom right). In stroma of the treated CNV, predominance score of VEGF to PEDF was significantly higher than in the control group (PS = 2, PS = 0, respectively, P = .0273).

• HISTOPATHOLOGICAL FINDINGS IN CNV AFTER A LONGER TIME INTERVAL FOLLOWING PDT TREATMENT: Of CNV extracted at longer post-PDT intervals (n = 11), CD34 positive vessels were detected in all but one membrane. In

tapraid3/zrx-ajopht/zrx-ajopht/zrx00806/zrx5377d06z | xppws | S=1 | 2/27/06 | 19:07 | Art: 5377 | DTD5.0

F4

AQ: 17

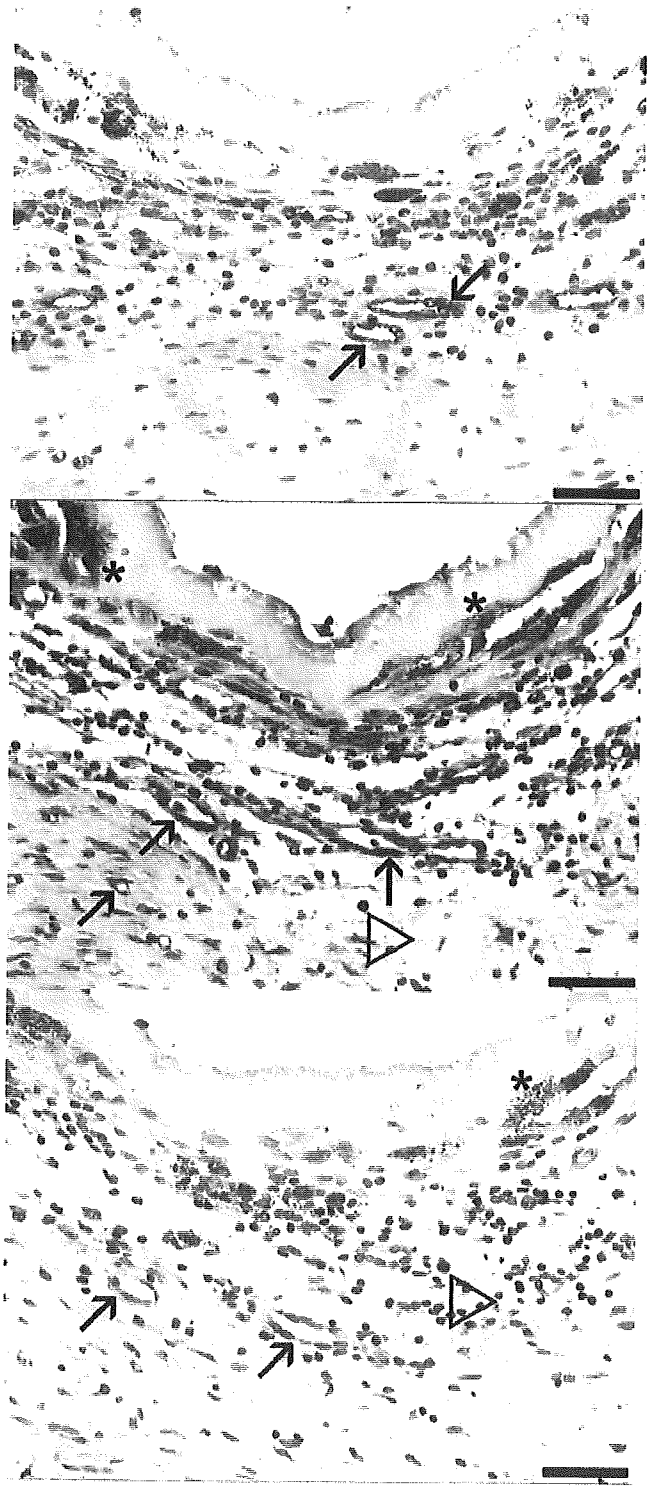

COLOR

FIGURE 4. Photomicrographs of a CNV membrane (patient 8 in Table) extracted 55 days after PDT. The serial sections were probed with CD105 (Top), VEGF (Middle), and PEDF (Bottom). (Top) Contrary to Figure 3, Top left, most of the vessels depicted by the brown chromogen are patent and lined with healthy activated endothelial cells (arrows). (Middle) retinal pigment epithelium Cells (asterisk), endothelial cells (arrows) and stromal cells (white arrow head) display VEGF strongly (red chromogen) but no PEDF (Bottom). A stromal cell, supposed to be an inflammatory cell, expresses PEDF (white arrow head) (red chromogen). Scale bars: 50 μm.

contrast to those in 3 day-old specimens, vessels were all patent and lined with endothelial cells displaying prominent nuclei. The specimens were highly vascularized. The vessels strongly expressed CD105 reflecting very vital and active endothelial cells. (Figure 4, Top) VEGF staining intensity was negative in only one case but moderate to strong at the vessels in 50% of the specimens. (Figure 4, Middle) Contrary to VEGF, vessels displayed PEDF expression in only four CNV (40%) and strongly in only two of them.

All but one membrane were extracted with retinal pigment epithelium cells as evidenced by CK18 staining (patient 11 in Table). Strong VEGF staining in retinal pigment epithelium persisted in 80% (8 of 10), being absent in only two cases (Figure 1, Top and Figure 4, Middle) and significantly higher than the control group ($P = .0007$). Retinal pigment epithelium cells expressed PEDF in 60% (6 of 10) of the specimens (n = 10) either weakly (30%) or strongly (30%) (Figure 1, Bottom). Predominance score of VEGF to PEDF in retinal pigment epithelium of the treated CNV persisted to be significantly higher than in the untreated CNV (PS = 1.5, PS = −1, respectively, $P = .0017$). Hypercellularity in stroma was found in 72.7% (8 of 11) of the specimens.

Stromal cells displayed VEGF in 91% (10 of 11) and PEDF in 54.5% (6 of 11) of the membranes. VEGF staining in stroma was mostly strong (6 of 10) or moderate (4 of 10), being weak in only one sample. Contrary to VEGF, strong PEDF expression in stroma was found in only one specimen (Figure 4, Bottom). Predominance score of VEGF to PEDF in stroma of these membranes persisted to be significantly higher than the control group (PS = 2, PS = 0, respectively, $P = .0263$).

In summary, VEGF staining was significantly increased in retinal pigment epithelium in CNV treated with PDT ($P < .0001$) whereas PEDF staining was significantly reduced in EC ($P = .0487$) and stroma ($P = .0081$) in PDT treated CNV. Predominance score of VEGF to PEDF was significantly higher in retinal pigment epithelium and stroma in treated CNV than in the control group ($P = .0004$, $P = .0053$, respectively).

DISCUSSION

HIGH RECURRENCE RATES FOLLOWING PDT COMPROMISE the benefits of the treatment. To reduce its limitations and use the possible adjuvant antiangiogenic treatments effectively, knowledge of impacts of PDT on angiogenesis in CNV is crucial.

Angiogenesis is controlled by the local balance between angiogenesis stimulatory and inhibitory factors.[19] Neovas-